SCIEPublish

Review

Solid Additives to Increase the Service Life of Ceramic Cutting Tool: Methodology and Mechanism

Yuxin Shi, Biao Zhao and Wenfeng Ding *

College of Mechanical and Electrical Engineering, Nanjing University of Aeronautics and Astronautics, Nanjing 210016, China; 2847385861@qq.com (Y.S.); zhaobiao@nuaa.edu.cn (B.Z.)

* Corresponding author. E-mail: dingwf2000@vip.163.com (W.D.)

Received: 20 June 2024; Accepted: 17 July 2024; Available online: 19 July 2024

ABSTRACT: With the development of the manufacturing industry, there is an increasing demand for high-efficiency processing, high-precision processing, and high-temperature processing. The characteristics of ceramic tools, such as high hardness and wear resistance, make them suitable for high-precision processing. Additionally, their excellent high temperature resistance perfectly meets the requirements of high temperature processing. However, ceramic tools have a relatively low strength and are prone to breakage, which limits their application in some high-strength machining fields. Their low toughness and brittleness also lead to easy cracking and reduced tool life, resulting in frequent tool changes that further limit processing efficiency. Therefore, improving the service life of ceramic tool materials is crucial to enhance processing efficiency and achieve significant economic benefits. With the development of material science, solid additives with toughening and strengthening properties have greatly improved the performance of ceramic tool materials and given ceramic tools new life-enhancing properties, such as lubrication and repair. By utilizing the combined action of one or more solid additives and employing surface coating technology, the service life of ceramic cutting tools is significantly extended. This makes the application of ceramic tools in industrial cutting more and more widely, and the demand is also growing rapidly. However, the mechanism and methods of various solid additives to increase the life of ceramic tool materials have not been systematically reviewed. The analysis of the composition and functional properties of ceramic tool materials was used as a basis to summarize the mechanism by which various solid additives improve the service life of ceramic tool materials, and to provide points for attention in their use. The aim is to assist researchers in designing and preparing new ceramic tool materials that can meet processing requirements. Finally, the research status, challenges, and prospects of enhancing the service life of ceramic cutting tools with solid additives are summarized, providing a foundation for further research.

Keywords: Ceramic tools; Self-lubrication; Self-repairing; Service life; Toughening and strengthening

1. Introduction

The manufacturing industry, as the fundamental sector of the national economy, exerts a profound influence on the country's development [1]. The advanced degree, quality, and performance of tools are directly linked to processing efficiency and subsequently impact economic benefits. Tools play a crucial role in metal cutting by facing significant challenges when machining various difficult materials at high speeds. Therefore, it is necessary to design and manufacture tools that meet processing requirements. As shown in Figure 1, ceramic tools have been put into use since 1950, and after a long time of development and optimization, by 2012, ceramic tools have shown a variety of advantages in practical applications. The researchers discovered that the utilization of additives as an effective method for enhancing the performance of ceramic materials can significantly enhance their wear resistance and damage resistance, thereby extending the service life of ceramic tools. This enables ceramic tools to meet the requirements for improving processing efficiency and promoting sustainable development in this field. Studying the impact of various solid additives on the service life of ceramic tools is beneficial for gaining a deeper understanding of how these additives work, providing a foundation for optimizing the performance of ceramic tools. Consequently, it facilitates efficient design of high-performance ceramic tools to meet industry and scientific technological development demands.

https://doi.org/10.35534/ism.2024.10009

The low fracture toughness of early mainstream ceramic cutting tool materials is the main reason for their poor reputation (Figure 2a), as it makes the cutting edge highly susceptible to fracturing, greatly restricting the practical application of ceramic materials [2]. In order to enhance the reliability of ceramic tool materials, researchers have utilized solid additives to increase their toughness and summarized the impact of mechanical properties on service life. While high hardness and strength typically result in good wear resistance, they also lead to low fracture toughness; conversely, high fracture toughness often results in lower hardness and increased susceptibility to wear. Therefore, even if reducing the hardness of a ceramic tool material can improve its fracture toughness, the addition of solid additives can restore or even enhance its wear resistance through strengthening effects. Additionally, these solid additives contribute to improved thermal fracture resistance of the tool material, which positively impacts reliability and service life. Consequently, it is necessary to optimize material's mechanical properties and design tough new ceramic tools in order to ensure their longevity.

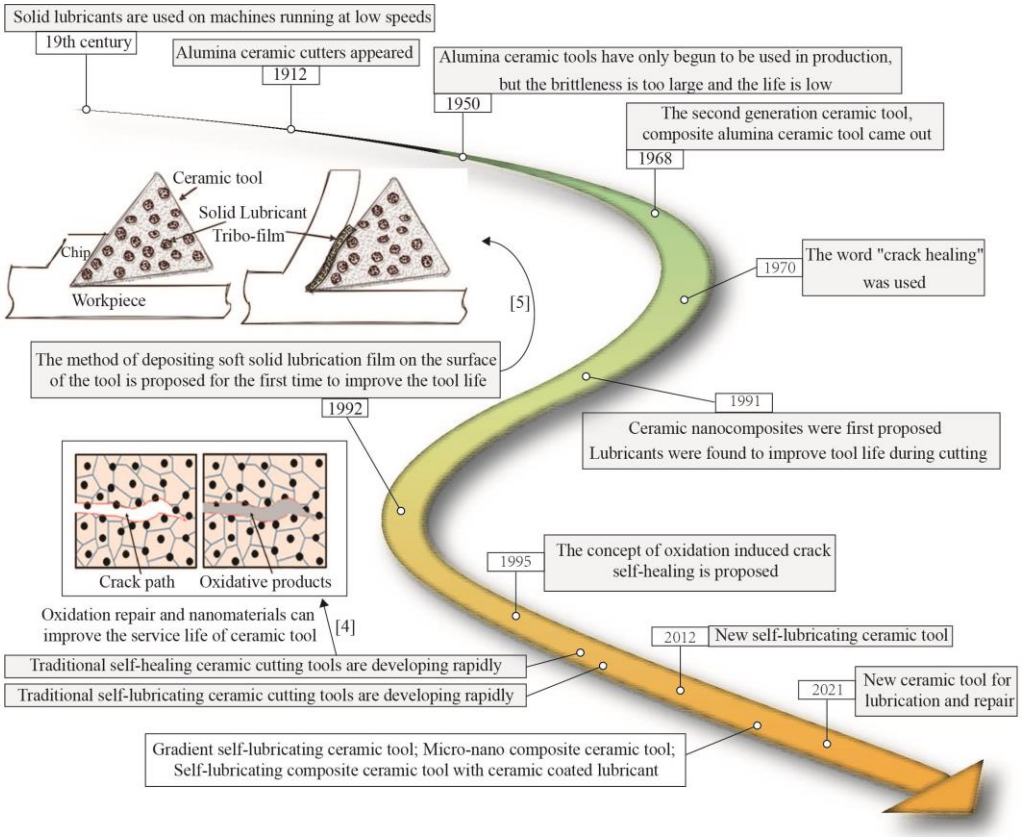

Figure 1. Ceramic tool development milestone [3–5]. Reproduced with permission from Elsevier.

The application of ceramic tools spans across various industries including aerospace, automotive, machining, and others (Figure 2b). Moreover, these tools can be precisely machined to yield exceptional quality products. As depicted in Figure 2c, researchers studying the practical application of new ceramic cutting tool materials have discovered that, in addition to their toughening and reinforcing properties [6], certain solid additive phases possess unique mechanisms for improving the lifespan of ceramic cutting tools. Some solid additives can create a lubrication layer on the surface of the tool, which reduces friction, minimizes tool wear, and enhances the longevity of ceramic tools [7]. This results in reduced maintenance and replacement costs during use, meeting application requirements in more extreme environments. Moreover, specific solid additives can react with oxygen and cause volume expansion of oxidation products. This expansion fills cracks, repairs micro-defects on material surfaces, hinders crack formation and propagation, ultimately leading to improved service life and reliability. Scholars have successfully combined restorative and lubricating effects using certain solid additives to enhance reliability and extend the service life of ceramic tools [8]. The self-healing properties of ceramic materials reduce safety accidents in aerospace and other fields, providing research ideas for engineers. However, recent studies indicate that fully harnessing the properties of these solid additives to improve ceramic tool lifespan necessitates specific usage environments. For instance, effective repair by solid agents is only achievable in high-temperature environments; carbon materials, some metal oxides, and certain transition metal disulfides lose their lubricating abilities at elevated temperatures, resulting in reduced friction; hBN, some metal oxides, and

alkaline earth metal fluorides require high-temperature conditions for generating lubrication effects and reducing friction. Therefore, the utilization requirements for ceramic tool materials should be thoroughly considered to avoid resource wastage.

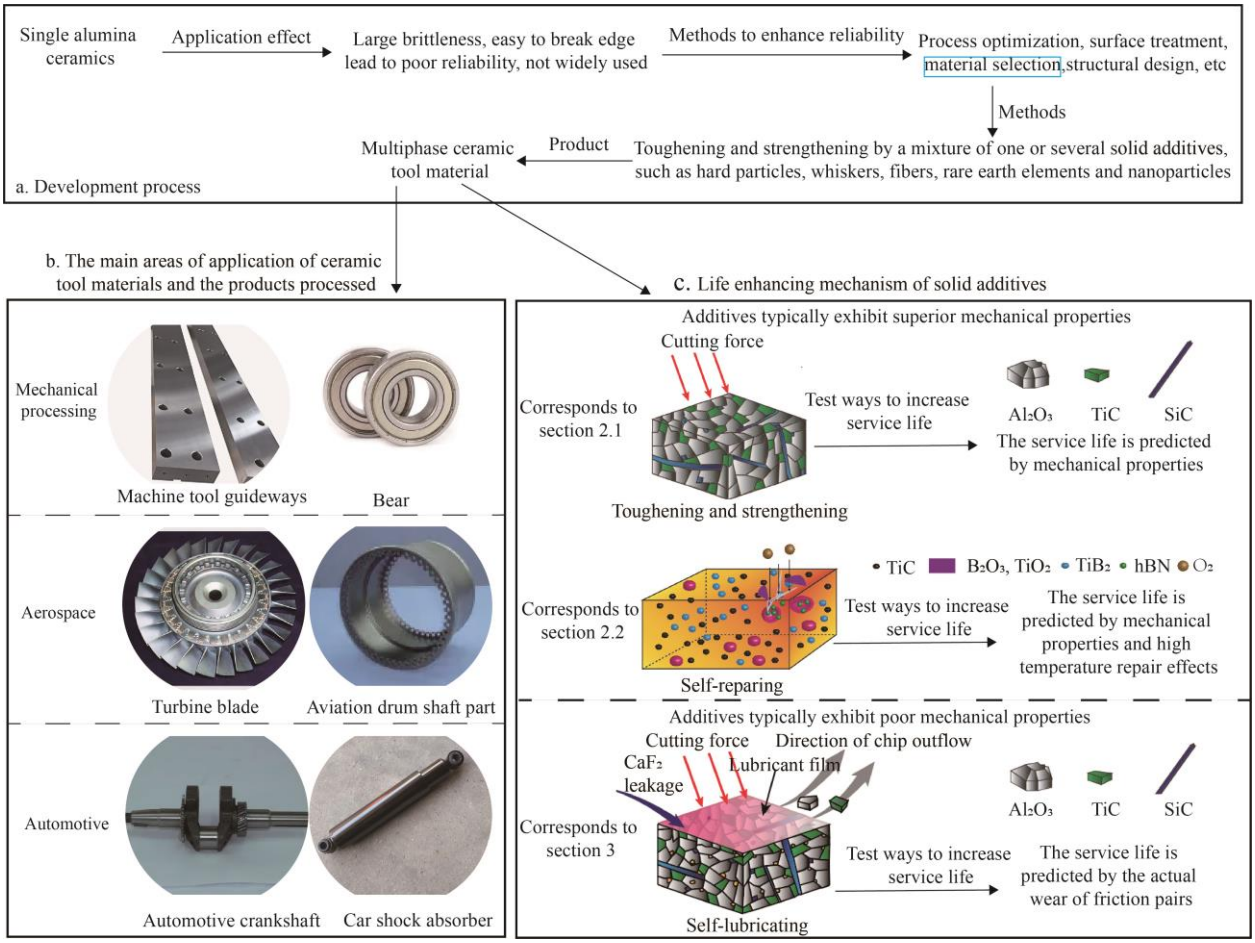

Figure 2. Key research elements [7].

This paper reviews the current state of research and prospects for development in the field of service life of ceramic tool materials both domestically and internationally. The mechanism and application considerations of various solid additives to enhance the service life of ceramic tool materials are examined. Additionally, the challenges faced by ceramic tool materials as well as current optimization options are discussed. Finally, research prospects for improving the service life of ceramic tool materials are presented. It is hoped that this review will deepen understanding of new ceramic tools and aid in designing the next generation of ceramic tool materials to meet machining requirements.

2. Methodology Studies

Ceramic tool materials are brittle, sensitive to surface defects, and prone to fracture at the cutting edge when impacted during the cutting process, significantly reducing their application reliability. Improving the reliability of ceramic tool materials can be achieved through material selection, process optimization, surface treatment, and structural design. Selection of suitable ceramic cutting tool material components is to improve the reliability of ceramic cutting tool material basis, embodied in the toughening and reinforcement to reduce crack initiation to hinder crack expansion, self-repair repair surface defects. In favour of the growth of the service life of ceramic tool materials [9,10].

2.1. Toughening, Strengthening Phenomenon to Increase the Service Life

In the field of machining, cutting tools play a crucial role as they significantly impact the surface quality of the workpiece. The characteristics of the cutting tool are closely related to this aspect. Ceramic tools have been widely adopted in industrial part production due to their superior wear and corrosion resistance compared to commonly used metal tools [2,11]. Additionally, ceramic tools possess excellent mechanical properties, making them suitable for processing high-strength difficult-to-machine materials [1]. However, single-phase ceramic tools have limitations; therefore, incorporating solid additives into the ceramic matrix can effectively enhance the overall performance of

ceramic tool materials and extend their service life [12]. Furthermore, utilizing solid additives can introduce new properties that broaden the application scenarios for ceramic tools.

The matrix phases and solid additives of ceramic materials are typically brittle and difficult to plastically deform, lacking mechanisms for depleting fracture energy. Therefore, the main toughening mechanism of composite ceramic materials is to enhance fracture toughness by increasing the ability of the crack extension process to deplete fracture energy [12–14]. Consequently, the toughening mechanism of composite ceramic materials is closely related to the crack extension mechanism. Ceramic materials are primarily toughened and reinforced by mixtures of one or several materials, such as hard particles, whiskers, fibers, rare earth elements, and nanoparticles. However, the type, content, size, and distribution of additives need to be rationally designed in order to significantly enhance the reliability and service life of ceramic tool materials.

2.1.1. Hard Particles

The presence of hard particles, as illustrated in Figure 3, can induce block cracking, leading to crack deflection, crack bridging, crack branching, and enhanced fracture toughness and flexural strength of the material. Good hardness with higher toughness and flexural strength greatly improves wear resistance and service life. Some carbides [15,16], nitrides, oxides [17–19], and borides [20–23] have been shown to improve the reliability of conventional ceramic tool materials [24,25]. Chen et al. [15] prepared WC to enhance the mechanical properties of Al_2O_3 nanocomposites, and found that the addition of WC accelerated the sintering process of Al_2O_3 matrix and improved its mechanical properties by hindering its grain growth. Song et al. [16] found that when the H_fC content increased from 15 wt% to 25 wt%, the pore number gradually decreased and the relative density gradually increased. The grain size of TiN and TiB_2 decreased, indicating that H_fC additive can inhibit the growth of TiN and TiB_2 grains and form fine structures which are conducive to improving the bending strength. The toughening mechanism of ceramics mainly includes H_fC grain pull-out, fine crystal, crack deflection and crack bridge. Because the hardness of H_fC is higher than TiN and lower than TiB_2, the increase of H_fC content increases the Vickers hardness of TiN-H_fC composite, but decreases the Vickers hardness of TiB_2-H_fC composite. According to the results of Yu et al. [17], as the volume fraction of ZrO_2 increases from 0% to 50%, the bending strength increases from 291 to 423 Mpa. Yazar et al. [21] showed that the fracture toughness of B_4C-SiC composites increased by 28% when 10% TiB_2 was added to the sample. Xia et al. [26] found that $TiSi_2$ mainly affected the intermediate sintering process of B_4C and increased the sintering rate, thus shortening the grain growth time and improving the comprehensive mechanical properties of the material. The results show that when the content of $TiSi_2$ is 10 wt%, the bending strength and fracture toughness of the composite ceramics are 807 MPa and 3.2 MPa·$m^{1/2}$.

The incorporation of hard particles, such as TiC or TiN, into the ceramic matrix enhances the material's hardness and wear resistance. However, at temperatures exceeding 800 °C, oxidation and subsequent degradation of titanium carbide and titanium nitride particles occur, resulting in a loss of their reinforcing properties [27].

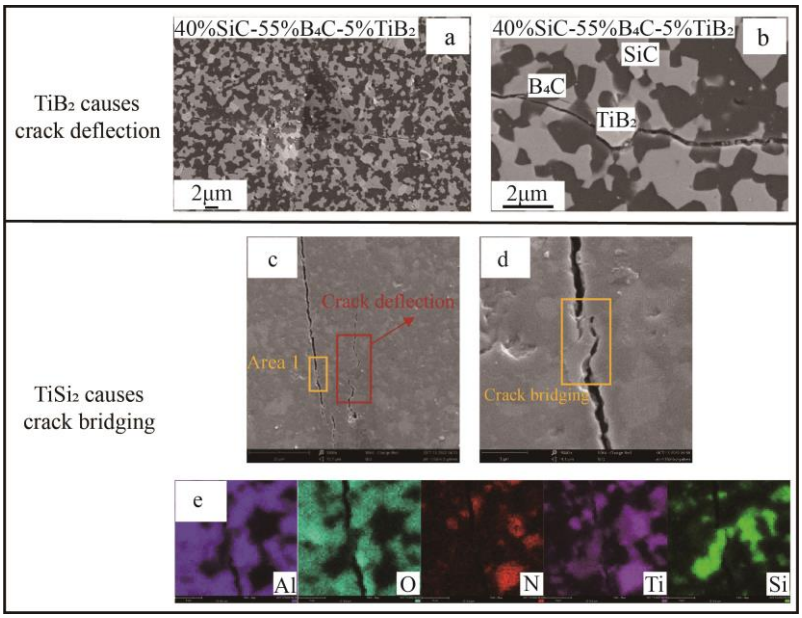

Figure 3. Crack deflection or crack bridging phenomenon due to hard particles [21,24]: (**a**,**b**) TiB_2 causes crack deflection; (**c**–**e**) $TiSi_2$ causes crack bridging. Reproduced with permission from Elsevier.

The addition of TiB_2 particles to the Al_2O_3 matrix by Deng et al. [28] resulted in notable improvements in fracture toughness, hardness, and flexural strength, leading to a significant enhancement in wear resistance and fracture behavior. The investigation unveiled that an increased content of TiB_2 demonstrated enhanced wear resistance.

Both sliding wear tests and cutting experiments exhibited reduced friction coefficient and wear rate for Al_2O_3/TiB_2 ceramic cutting tool materials with varying TiB_2 contents (0–40 vol%). However, it is worth noting that the high temperature oxidation of TiB_2 generates B_2O_3 which can easily volatilize [29], potentially negatively impacting the material's flexural strength and reliability. Therefore, in the actual processing application, the processing temperature to ensure the life of ceramic tools is an important factor.

Skopp et al. [30] added TiN or BN to Si_3N_4, which significantly reduced the wear rate. They concluded that in order to improve the wear resistance of conventional Si_3N_4 ceramics, glassy phases should be minimized as much as possible and thermal dispersion and thermal conductivity should be increased to reduce thermal stresses and prevent thermal cracking. Ko et al. [31] found that the optimal content of SiC in Al_2O_3 ceramics varies when machining different workpieces. The tool life of Al_2O_3-10 wt% SiC composite tool was the longest when machining heat-treated AISI 4140 steel, which was 7 times longer than that of Al_2O_3-TiC composite tool, while a 5 wt% SiC composite tool was the longest when machining grey cast iron. It can be observed that the service life of ceramic tool materials is not solely determined by mechanical properties but is closely related to the actual machining application environment.

2.1.2. Nanomaterials

The presence of nanophase alters the mode of crack propagation in single-phase ceramic materials, transforming it from a solely along-crystal fracture to a hybrid fracture where both through-crystal and along-crystal fractures coexist [32–34]. The location of the nanophase has a significant influence on the material properties, which is also of additional interest [3,35,36]. This consumes more fracture energy and improves fracture toughness [37,38]. The dispersion of carbon nanoparticles in the matrix, the interface bonding state with the matrix and the structural change are the main reasons for the strengthening and toughening of carbon nanoparticles [33]. Yi et al. [34] found that nanoscale CaF_2-induced transgranular fracture enhanced the toughness of the composite. Crack flexure is the main toughening mechanism of nanometer CaF_2 composites. Mustafa et al. [35] pointed out that compared to alumina, The strength and toughness of alumina composites containing 1.5 wt% multi-walled carbon nanotubes (MWCNTs) increased by 58% and 66%, respectively. Liao et al. [36] found that Si_2BC_3N ceramics doped with 1 vol% MWCNTs had higher bending strength and fracture toughness. The toughening and strengthening effect of 462.1 MPa and 5.54 $MPa \cdot m^{1/2}$ is mainly due to the highly energy-intensive bridging and drawing.

By investigating the toughening mechanism of Al_2O_3 ceramics reinforced with nano-ZrO_2 additives, Du et al. [39] found that the nanophase inside the Al_2O_3 crystal plays a dominant role in altering the fracture mode of nanocomplex ceramic materials. The ZrO_2-Al_2O_3 composite ceramics (ZTA-1), prepared through mechanical grinding and dispersion methods, exhibit a significant presence of "intracrystalline" structures, as depicted in Figure 4a–f. These structures offer more convoluted crack deflection paths and consume higher fracture energy compared to conventional ceramics obtained via direct powder doping (ZTA-2). Consequently, the flexural strength and fracture toughness exhibited a significant enhancement of 50% and 83%, respectively. This observation suggests that the incorporation of nanoparticles within the crystal lattice is imperative for achieving superior outcomes. To summarize the mechanism, the presence of an "intracrystalline" structure gives rise to the formation of subgranular boundaries within the Al_2O_3 particles, resembling a re-refinement of their organization and resulting in reinforcement through small particle effects. As shown in Figure 4g,h, W_2C/Al_2O_3 nanocomposites exhibit only crack deflection, while WC/Al_2O_3 nanocomposites exhibit crack bridging, crack deflection, and secondary cracking. The additional mechanism provided by WC with small particles to absorb the fracture energy leads to an increase in the overall mechanical properties of the material.

The effect of TiC nanoparticles on the mechanical properties of Al_2O_3/SiC_w materials was investigated by Zhao et al. [40]. It was observed that the incorporation of nanoparticles significantly enhanced the bending strength, thermal hardness, and high temperature fracture toughness of Al_2O_3/SiC_w ceramic tool materials at room temperature. However, at high temperatures, these composites were prone to fracturing along the crystal structure, resulting in low high-temperature bending strength for $Al_2O_3/SiC_w/TiC_n$ composites. This hindered the improvement of high-temperature bending strength. Yin et al. [41] prepared ceramic tools containing both TiC nanoparticles and micron-sized TiC particles in an alumina-based matrix for machining austenitic stainless steel. They discovered that these tools exhibited superior wear resistance compared to alumina-based ceramic tools enhanced only with micron-sized TiC particles. The use of nanoparticles enhanced tool life.

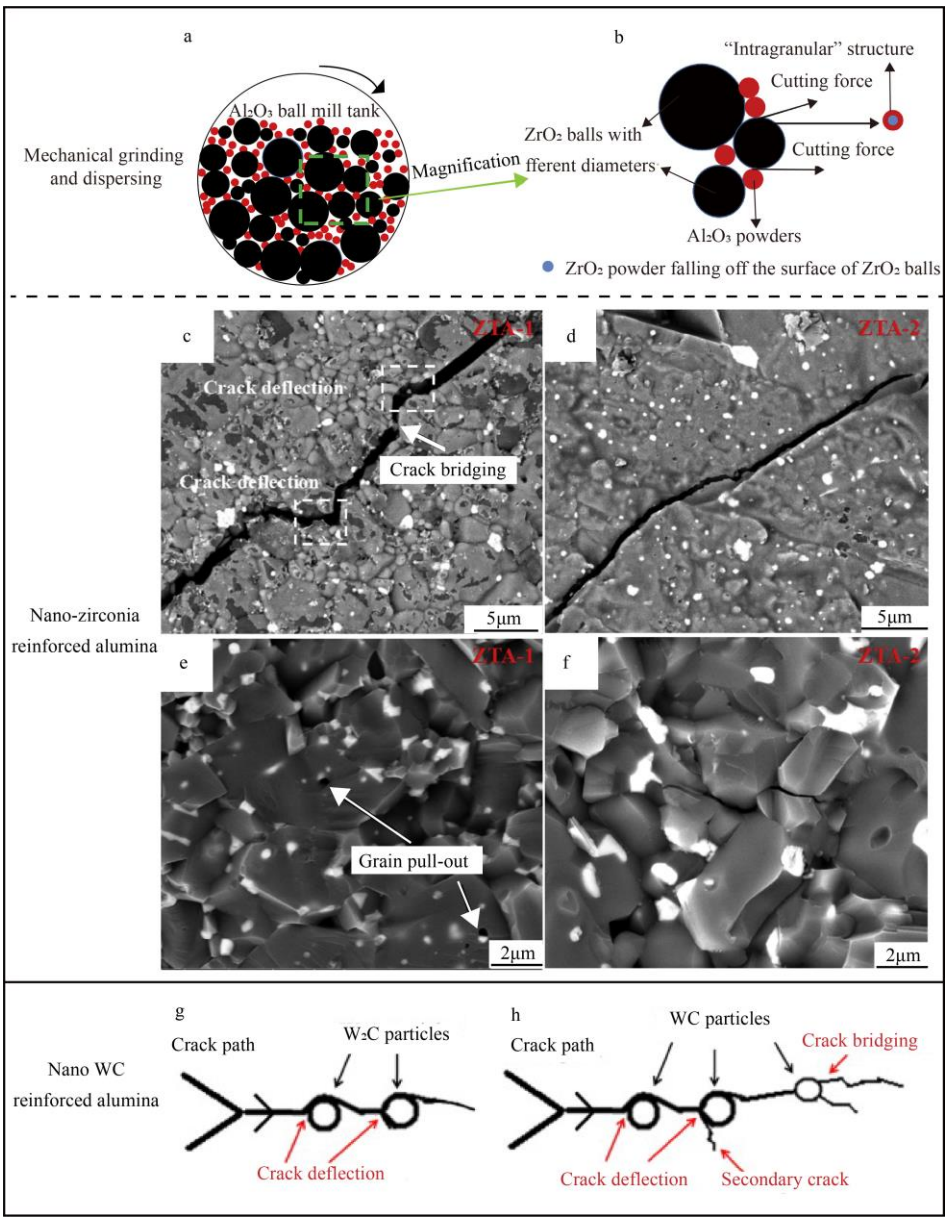

Figure 4. Nanoparticle reinforced ceramic tool materials [15,39]: (**a**,**b**) The simulation diagram illustrating the mechanical grinding and dispersion technology; (**c**–**f**) The crack propagation path and fracture morphology of ZTA composite ceramics obtained through two distinct powder preparation methods; Schematic representations of crack fracture paths in (**g**) W_2C/Al_2O_3 and (**h**) WC/Al_2O_3 nanocomposites. Reproduced with permission from Elsevier.

2.1.3. Whiskers and Fibres

Adding whiskers [42,43] or fibers [44,45] to the ceramic matrix can improve the fracture toughness of the material through crack branching, bridging and flexural behavior [46,47]. Yu et al. [42] introduced mineral bridging agent, and the bending strength and fracture toughness of aluminum-based ceramics were increased by 33.97% and 33.52%, respectively. More crack deflection, crack bridging and whisker pulling out occurred on the fracture surface. Zhu et al. [43] found that the introduction of SiC whisker could significantly improve the mechanical properties of SiCO ceramics. When the SiC whisker content varies from 0 to 5 wt%, the bending strength of the sample increases from 44.2 ± 4.1 MPa to 260.1 ± 49.7 MPa. The fracture toughness increased from 1.48 ± 0.03 $MPa \cdot m^{1/2}$ to 3.23 ± 0.12 $MPa \cdot m^{1/2}$. The mechanism of SiCO ceramic SiC whisker toughening mainly includes whisker breaking and pulling out, deflection, crack bridging, directional distribution of whisker and compressive stress of SiC whisker on ceramic matrix. Chen et al. [44] constructed polycrystalline cubic boron nitride/hexagonal boron nitride (PcBN/hBN) fiber monolithic ceramics with long fiber arrangement structure using cubic boron nitride/hexagonal boron nitride (PcBN/hBN) fiber as the grain boundary. The failure of composite ceramics was non-brittle, which was mainly attributed to the multi-scale crack effect in the layered structure. The maximum crack propagation toughness is extremely high (about 21 $MPa \cdot m^{1/2}$), which is 270% higher than the crack initiation toughness. Lang et al. [47] significantly strengthened and toughened porous Yttria-

stabilized zirconia (YSZ) by using Al_2O_3 fiber. When the addition of Al_2O_3 fiber was 10 vol%, the strength of porous YSZ ceramics reached the maximum, with a compressive strength of 100.2 ± 25.4 MPa. The bending strength is 61.5 ± 11.3 MPa. With the increase of Al_2O_3 fiber content, the fracture toughness of YSZ ceramics increased monotonously, from 0.5MPa·$m^{1/2}$ to 1.2MPa·$m^{1/2}$, an increase of 140%.

A large number of researchers have revealed the toughening mechanism of SiC fibers by studying the crack extension mode of SiC_f/SiC composites. When the applied load is large, the ceramic matrix will crack earlier than the fibers [48,49]. Under continuous loading, cracks in the matrix extend to the matrix-fiber interface, resulting in two different scenarios [50,51]. In cases where the bond strength at the matrix-fiber interface is weak, cracks propagate along the interface and bypass the fibers. Conversely, when there is a strong bond at this interface, cracks propagate through or around individual fibers. Regarding how crack extension modes influence properties of fiber-reinforced ceramic matrix composites, Yang et al. [52] explained their connection with material properties from an interfacial bond strength perspective. The length of fiber pull-out demonstrates this bond strength at the matrix-fiber interface. When interfacial bond strength between fiber and matrix is weak, it hampers effective transfer of applied load from fiber to matrix and reduces overall strength of SiC_f/SiC material; conversely, when interfacial bond strength between fiber and matrix is very high, it does not favor manifestation of overall toughness in SiC_f/SiC material.

Huang [2] and Jia [8] employed silicon carbide whisker (SiC_w) reinforcement to fabricate ceramic tools exhibiting enhanced flexural strength, fracture toughness, and resistance to cutting wear. Guo et al. [53] and Liu et al. [54] used Al_2O_3-reinforced ceramic tools with SiC_w to machine Inconel718 parts, which exhibited good machinability. The toughening mechanism of SiAlCN ceramics reinforced by SiC whiskers or graphene nanoparticles (GNPs) was investigated by Li et al. [55]. As depicted in Figure 5, the high fracture toughness of SiAlCN ceramics is attributed to alternating along-crystal and through-crystal fractures combined with grain bridging. The toughening mechanisms of SiC_w/SiAlCN and GNP/SiAlCN ceramics exhibit similarities, encompassing crack deflection, bridging, and pullout; however, their frequencies of occurrence and effects manifest distinct variations. Due to the strong interfacial bonding between SiC_w and SiC grains, crack deflection induced by SiC_w is limited, while the pull-out length is reduced without any occurrence of crack branching phenomenon; thus slightly enhancing the toughness of SiC_w/SiAlCN ceramics. The GNP/SiAlCN ceramics exhibit enhanced fracture toughness compared to other materials due to a larger specific surface area and improved interfacial bonding between GNPs and the matrix, which facilitates effective toughening mechanisms such as crack deflection/branching and GNP bridging/pull-out. It is evident that bond strength between fibers/whiskers/nanoparticles/matrix has a significant influence on material properties.

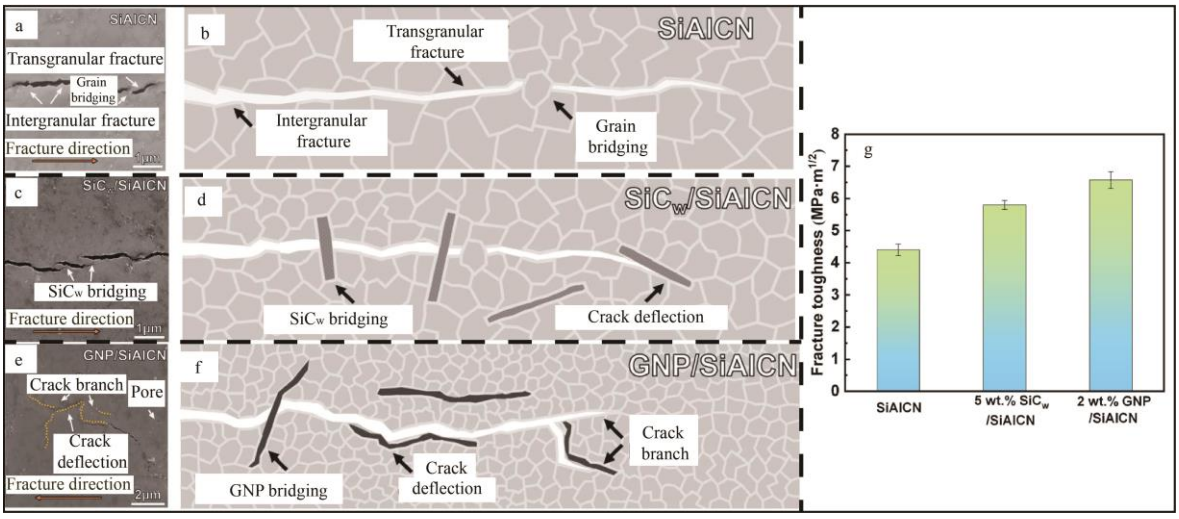

Figure 5. Schematics illustrating toughening mechanisms: (**a**) Crack propagation in SiAlCN ceramic; (**b**) Toughening mechanism of SiAlCN ceramic; (**c**) Crack formation in SiC_w/SiAlCN ceramic; (**d**) Toughening mechanism of SiC_w/SiAlCN ceramic; (**e**) Crack deflection and branching in GNP/SiAlCN ceramic; (**f**) Toughening mechanism of GNP/SiAlCN ceramic; (**g**) Fracture toughness comparison among SiAlCN, SiC_w/SiAlCN, and GNP/SiAlCN ceramics [55]. Reproduced with permission from Elsevier.

Zhao et al. [56] discovered that TiC nanoparticles within Al_2O_3 particles can induce perforation fracture and deflect cracks, thereby synergistically enhancing the overall performance of the material when combined with whiskers. Zhang et al. [7] incorporated SiC whiskers and particles into the matrix, improving their reliability significantly. Therefore, the collaboration between whiskers and nanoparticles or hard particles can result in ceramic tool materials exhibiting

enhanced overall performance. Whiskers and nanoparticles or hard particles demonstrate a synergistic toughening or strengthening mechanism, thereby enabling the achievement of ceramic tool materials with exceptional performance.

2.1.4. Rare Earth Elements

The utilization of rare earth elements has become indispensable in the preparatory procedure of novel ceramic tool materials. The incorporation of rare earth elements can enhance the sintering process of ceramics, while the addition of a mixture of these elements reduces porosity in composites and optimizes the microstructure of ceramic cutting tool materials, thereby improving performance and extending service life [57–59].

Xu et al. [60] found that the action mechanism of Y element additive was mainly to purify the interface, thereby improving the binding strength of the interface and strengthening the effect of nano-sized particles. Due to the coexistence of strong interface and weak interface, the synergistic effect of crack bridging, crack branching, crack defects and micro-cracks was enhanced. Zhang et al. [57] incorporated a blend of rare earth elements (RE), namely Nd, Ce, La, and Pr, into the Al_2O_3 matrix to investigate the influence of this mixed rare earth element addition on properties and microstructure. The addition of RE improved the mechanical properties, as demonstrated in Table 1. The pure alumina particles, as shown in Figure 6a, exhibited irregular shapes and abnormal growth, with the fracture mode primarily being along-crystal fracture. As shown in Figure 6b,c, although the fracture mode did not change, the addition of mixed rare earths resulted in uniform size and regular shape of alumina particles and additive particles in the composites.

Table 1. Material components and mechanical properties [57].

Sample	Compositions (vol%)	Hardness (GPa)	Bending Strength (MPa)	Fracture Toughness ($MPa \cdot m^{1/2}$)
1	100% Al_2O_3	17.84	130.0	3.13
2	0.5% RE + 99.5%Al_2O_3	17.96	247.0	3.52
3	2% RE + 98% Al_2O_3	18.73	303.5	3.76

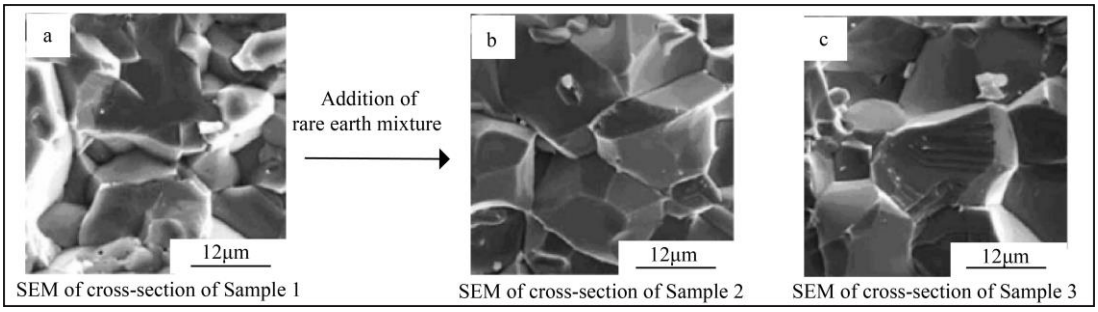

Figure 6. Influences of rare earth elements on the microscopic morphology of materials [57]: (**a**) SEM of cross-section of sample 1; (**b**) SEM of cross-section of sample 2; (**c**) SEM of cross-section of sample 3. Reproduced with permission from Elsevier.

Rare earth elements are widely used as effective additives in current research on advanced ceramic materials [61,62]. They serve not only as stabilizers for tetragonal zirconia but also as sintering aids for ceramics such as Al_2O_3, TiB_2, TiC, SiC, Si_3N_4, Sialon and AlN [63,64]. The mechanical properties of all these ceramic materials can be significantly enhanced. Using yttrium oxide as a liquid phase sintering agent, Kennametal introduced their syalon ceramic tool [65]. Choi et al. [66] prepared Yb/Y co-doped SiAlON ceramics using rare earth oxide Yb_2O_3 as the main sintering additive. Intercrystalline fracture was predominantly observed in the Yb/Y co-doped SiAlON ceramics in terms of crack propagation. The fracture toughness increased by 53.6% from 4.6 to 7.0 $MPa \cdot m^{1/2}$, and the content of sintering additives was optimized.

Qiu et al. [67] found that the addition of different amounts of Y_2O_3 or CeO_2 to Al_2O_3 ceramics could significantly reduce the sintering temperature and greatly improve the material properties. Xu et al. [17,68] utilized Y-reinforced Al_2O_3/(W, Ti)C ceramics and observed that the maximum flexural strength and fracture toughness were approximately 20% higher compared to those of the corresponding materials without added Y element. The researchers concluded that the primary mechanisms of action exhibited by the Y element additive encompass interface purification, enhancement of interface bonding strength, and nanoparticle augmentation. After machining hardened 45 carbon steel and HT20-40 cast iron, it was found that the wear resistance of the new tool was superior to that of the corresponding material without

rare earths. The improvement in cutting performance of Al_2O_3/(W, Ti)C ceramic tool materials by rare earth elements was achieved through enhancing their microstructure and mechanical properties. Therefore, high-performance structural ceramics, such as fully stabilized zirconia ceramics (FSZ), tetragonal zirconia polycrystals (TZP), and other high-performance structural ceramics, can be synthesized by incorporating various rare earth oxides in different types and quantities. The addition of rare earth oxides not only suppresses the phase transition of the ceramics but also improves their flexural strength and toughness. Adding rare earth oxides as additives, stabilizers, and sintering aids greatly enhances the performance and extends the service life of advanced ceramics.

2.2. Self-Repairing Phenomenon Increases Service Life

The most intuitive effect of the self-repairing phenomenon of ceramic tool materials is the improvement of service life. During the preparation and machining of ceramic tools, defects such as porosity and microcracks can occur [69], which can lead to a decrease in the mechanical properties of ceramic tools, making them more susceptible to wear or fracture failure in the process of use, and decreasing the service life of ceramic tools. Therefore, processes to eliminate surface defects are very important to safeguard the performance and lifetime of ceramic materials. Such as grinding, polishing and heat treatment. In order to reduce defects such as surface porosity and microcracks, ceramic materials are prevented from premature failure due to surface damage [70]. A significant number of scholars have improved the service life of ceramic tools through the self-repair function of ceramic materials [4,71], showing that self-repairing ceramic tools can effectively utilise the heat of cutting to produce a liquid phase that fills the cracks and achieves crack self-repairing.

Researchers have classified the self-repairing mechanisms and repair methods of ceramic materials into three types: adsorption repair, chemical reaction repair, and diffusion repair. Adsorption repair has a low treatment temperature but limited repairing effect [71,72]. The temperature for diffusion repair needs to be close to the sintering temperature [73,74], which consumes excessive resources. Therefore, chemical reactions are primarily used for repairing surface defects during the actual cutting process [75,76]. However, when using chemical reactions for surface defect repair, attention should be paid to the impact of repair temperature and reaction products on the effectiveness of the repair.

Gupta et al. [71,77,78] discovered that MgO and Al_2O_3 ceramic materials can undergo crack self-repair through annealing treatment. After conducting numerous experiments, researchers discovered that materials such as Al_2O_3, Si_3N_4, SiC [79–81], BC_4 [82], ZrB_2 [83], ZrN [84], mullite [85], MAX materials, (e.g.: Ti_2AlC, Ti_3AlC_2) [86,87] and their composites [88–91] exhibit a phenomenon of self-repairing cracks. Chu et al. [92] found that amorphous silica formed by oxidation of silicon and silicon carbide could fill cracks and heal cracks. Houjou et al. [93] found that the cracks of Si_3N_4/SiC composite ceramics completely healed in air, but did not heal in argon, N_2 gas and vacuum. Wang et al. [94] found that the cracks of SiC-Al_2O_3-B_4C ceramics could be completely healed in the air above 700 °C. The ceramic composite material had the best effect when repaired at 700 °C for 30 min, and its bending strength could be restored to 94.2% of the original. Self-repairing ceramic materials can restore the attenuation strength caused by cracks and other micro-defects after heat treatment [95–98]. Yoshioka et al. [95] determined the lowest temperature at which the strength of the crack healed sample of Mullite /$TiSi_2$ composite recovered to the strength of the unbroken sample, and determined it to be 600 °C. Burlachenko et al. [96] found that regardless of SiC content, ZrB_2-SiC ceramic composite had the best defect self-healing effect after annealing at 1600 °C. Monteverde et al. [97] found that silica glass phase generated by SiC oxidation had a repairing effect. Dedova et al. [98] found that the thickness of the oxide layer of the ceramic composite (ZrB_2-ZrC-SiC)-ZrO increased with the increase of the volume fraction of zirconia, and that the temperature of 1600 °C had a complete healing effect on the defects of the ceramic composite regardless of the content of ZrO_2.

Furthermore, they can even eliminate residual stress while achieving complete crack repair [99], thereby enhancing the mechanical properties of the material and bolstering the reliability of ceramic materials. However, it should be noted that subjecting some materials to high heat treatment temperatures can result in the formation of porosity, which adversely affects their performance [100]. Shi et al. [24] used $TiSi_2$ to reduce the porosity of the repair surface and reduce gas volatilization (Figure 7).

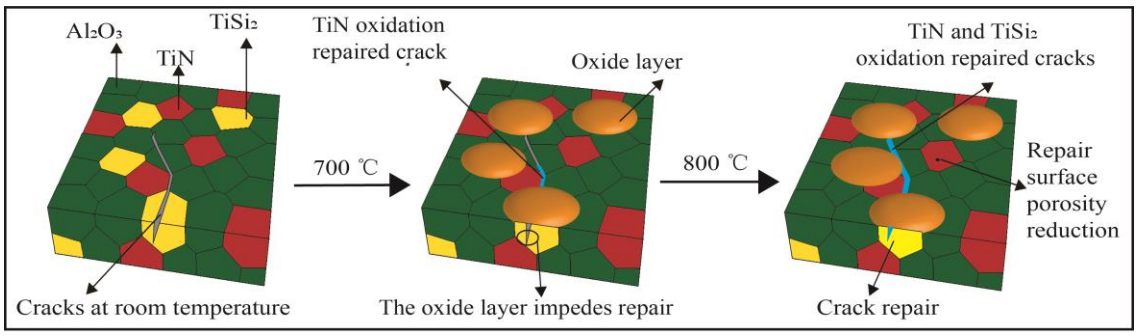

Figure 7. Mechanism diagram of $TiSi_2$ reducing and repairing surface porosity [24]. Reproduced with permission from Elsevier.

A significant number of scholars [101–103] have investigated the repairing effect of Al_2O_3/SiC nanocomposite ceramics and have discovered that heat treatment at temperatures ranging from 1273 K to 1773 K can effectively repair cracks measuring less than 250 μm in length and no more than 100 μm in depth. The room-temperature flexural strength of Al_2O_3/SiC nanocomposite ceramic materials can be fully restored. It is worth noting that if the cracks are repaired by transporting the glass phase generated in a high-temperature environment to them, then the ceramic material used for repairing will soften at high temperatures, thereby reducing its strength [73]. However, if the self-repairing phenomenon can promote the precipitation of the glass phase at the fracture, it will improve the high temperature strength of the ceramic material. Therefore, not only does the self-repairing function of ceramics cracks [104–106] help restore material strength, but it also enhances mechanical strength, thereby increasing lifetime and reliability. Takahashi et al. [107] and Ando et al. [92] studied the self-repairing effect of Al_2O_3/SiC_w and Si_3N_4/SiC The effect of self-repairing of ceramic materials was investigated at 1300 °C. It was found that the room temperature fatigue strength of ceramic materials after crack repair was restored to that of the original smooth specimen, and the static fatigue strength of Si_3N_4/SiC was also comparable to that of the original smooth specimen at 1000 °C, which indicated that the fatigue strength in the region of self-repairing was better restored.

Liu et al. [108] investigated the repair effect of Mullite/ZrO_2/SiC_p after heat treatment at 800 °C and found that the cracks on the material's surface were almost completely repaired, and the fracture toughness of the material recovered. However, due to the sensitivity of bending strength to surface defects, there is no significant recovery in strength. Sun et al. [109] found that the smaller the particle size of Al_2O_3-MgO composites, the better their repairing ability. The self-repairing properties of alumina ceramic materials containing SiO_2 and MgO were investigated by Moffatt et al. [110]. It was observed that the fracture toughness gradually increased with increasing heat treatment temperature. However, a significant decrease in fracture toughness was observed when the temperature reached 800 °C. This is because the inflow of intergranular glass phases into the cracks to achieve the material repair will lead to the material softening phenomenon in the high temperature environment. However, for Al_2O_3-17 vol% SiC ceramic materials, the room temperature fracture toughness reaches its maximum value when the repair temperature reaches 1200 °C, and there is no significant decrease in the fracture toughness with the increase of the test temperature. Savchenko et al. [111] observed in the friction experiment of ZrB_2-20 vol% SiC ceramics that liquid borosilicate glass has the self-repairing effect of subsurface defects. This is because the low shear resistance viscous mechanical mixed layer composed of borosilicate glass, trioxide and transfer products can reduce friction, repair subsurface cracks, and keep the wear rate at an acceptable level.

Cui et al. [112] prepared $Al_2O_3/TiC/TiB_2$ (ATB) ceramic tools and discovered that the cutting heat during the cutting process enabled the tools to repair certain micro-defects, thereby enhancing their tool life. As depicted in Figure 8, TiB_2 oxidation caused by the cutting heat is identified as the primary factor contributing to tool restoration during cutting.

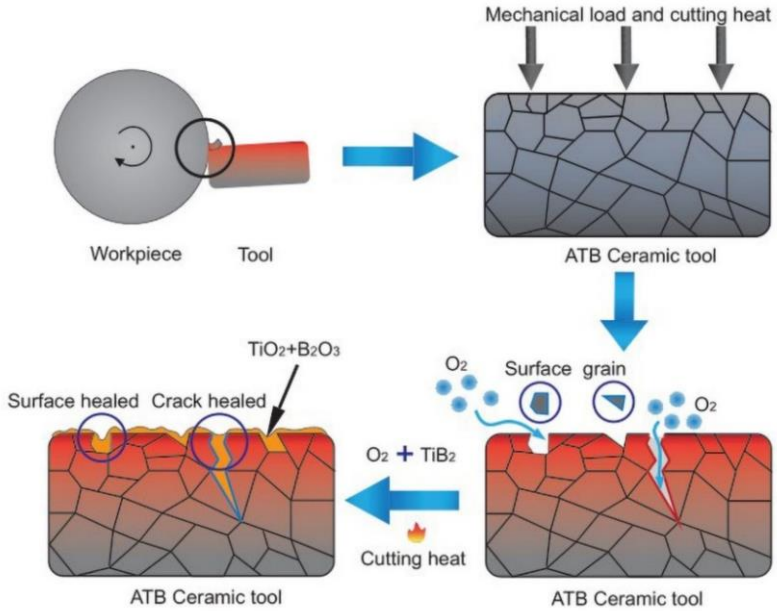

Figure 8. A schematic diagram of the repair function of ATB tools during cutting [112].

Zhao et al. [113] investigated the cutting performance of a ceramic tool reinforced with whiskers and nanoparticles ($Al_2O_3/SiC_w/TiC_n$) for dry cutting Inconel718 and high-speed machining of Inconel718. The new ceramic tool can be reliably used at high speeds up to 400 m/min. The tool material undergoes oxidation to a glassy phase at a high temperature of 1200 °C, which repairs thermal cracks on the tool edge, inhibits crack expansion, prevents instant damage to the tool, and assists in improving its lifespan. Shi et al. [8] investigated the Al_2O_3/TiC/10 vol% TiB_2/5 vol% hBN@Al_2O_3 (AT10B@5) ceramic. The cracks were partially repaired by the addition of B_2O_3 and TiO_2 during dry turning of 40Cr hardened steel. This filling process effectively prevented the accumulation of micro-cracks in the ceramic tool material during cutting, thereby reducing the risk of brittle fracture. As a result, tool wear was reduced and tool life was extended.

Some scholars evaluated the service life of ceramic tool materials through simulation [114]. A constitutive model was developed to analyze the behavior of self-healing ceramic materials in a finite element framework. Ozaki et al. [115] proposed a damage repair constitutive model for self-healing ceramics, incorporating an oxidation kinetics-based crack repair behavior evolution law. The time-dependent relationship of strength recovery obtained by finite element analysis is quantitatively compared with the reported experimental data of Al_2O_3/15 vol% SiC particles, Al_2O_3/30 vol% SiC particles and monolithic SiC. The findings demonstrate that the finite element analysis method employed in this study effectively replicates the fundamental characteristics of strength recovery observed in self-healing ceramics. Maeda et al. [116] used this model and finite element method to calculate the self-healing properties of surface cracks, and the results showed that the method could estimate the healing conditions and verify the stress by obtaining the microstructure information and oxidation kinetic parameters of ceramic components in advance. Bellezza et al. [117] proposed a model for predicting the tensile life of self-healing, long SiC fiber-reinforced ceramic matrix composites in an oxidizing environment. The model can accurately describe the physical and chemical phenomena of the crack with time, especially the oxygen concentration field, the degradation of the reactive matrix layer and the formation of related oxides, and the oxidation of the interface around the fiber.

In the machining process is a dynamic process, the surface will continue to be damaged, repair speed is an important parameter. The effectiveness of TiC restorers in the low-temperature self-healing behavior of Al_2O_3-based self-healing ceramics was evaluated by Nakao et al. [118]. The 30% TiC-70% Al_2O_3 intermediate layer was the best restorers for self-healing ceramics, and good healing effect could be achieved within 10 min at 600 °C. A successful development of a prototype for low pressure turbine blades has been achieved, featuring fiber reinforced self-healing ceramics. However, there are few studies on the repair rate, and a few scholars make up for the lack of relevant data through simulation [115]. Some researchers have looked at ways to increase the rate of repair. Greil [119] accelerates crack filling by reducing the healing agent particles to the nanoscale, forming a low viscosity polysilicate or borate melt phase and forming a solid solution, thereby reducing the healing temperature and shortening the healing time. Huang et al. [120] found that the synergistic effect of oxidation-induced healing and precipitation-induced healing of SiC particles and whiskers could indeed improve the crack repair rate and oxidation resistance of sic coatings. This collaborative

repair mechanism may broaden the potential applications of existing self-healing ceramic coatings in high-temperature oxidation environments. Through the above research, it can be seen that the repair speed is an important factor affecting the service life of ceramic tools in actual machining engineering. There are few experimental data on the repair speed of various repair agents. Collaborative repair is an effective method to improve the repair speed.

3. Mechanism Increase Service Life

The high levels of friction experienced at the tool-workpiece interface during the cutting process give rise to excessive heat, leading to elevated local temperatures of the tool owing to the limited thermal conductivity exhibited by ceramic tools. This can lead to severe wear or even fracture in that specific area [121], significantly reducing the service life of ceramic tools. The addition of an appropriate amount of solid additive phase, which can provide the tool with a friction-reducing effect, can reduce cutting heat, decrease wear, and extend the tool's lifespan. These solid additives mainly include self-lubricating additives and some sintering additives. The former method relies on the formation of a lubricant layer between the tool and the workpiece, effectively separating them and thereby reducing friction. Conversely, the latter approach is based on optimizing the crystal structure of ceramic tool materials to minimize friction. Although extensive research has been conducted on these corresponding solid additives in various fields [122–124]. Since powder metallurgy is the most commonly used synthetic technology for manufacturing inserts, the sintering temperature of ceramic tool materials is mostly higher than 1300 °C. This exceeds the decomposition temperatures of some metallic disulphides (MoS_2, WS_2), Ag_2MoO_4 [125–127], etc., which can be applied in certain ceramic coatings or surface weaves, and other substrates [128] but are difficult to directly become solid additives for ceramic tool materials. The main additives applied in ceramic matrix are as follows.

Carbon materials such as graphene [129] and carbon nanotubes [130], metal oxides (e.g., Cu_2O, B_2O_3, MnO_2, ZnO, MgO), fluorides (e.g., BaF_2, CaF_2) [131,132], hexagonal boron nitride (hBN), and Ti_3SiC_2 [133] are studied.

However, the properties of solid additives in ceramic tool materials needs to be considered in terms of sintering temperature, substrate material properties, solid additive properties and dosage, as well as the environment in which they are used. For example, the Cu663 substrate has low hardness and poor bonding with graphite. Adding only a small amount of graphite can provide good lubricating properties. However, when the graphite content is lower than 15 vol%, it becomes difficult to achieve effective lubrication in alumina-graphite composites, which may lead to rapid degradation of the material's mechanical properties [134–136]. Carrapichano et al. [134] found that silicon nitride materials could benefit from the addition of boron nitride tablets only when a small amount (10 vol%) of boron nitride tablets were added, thus improving their tribological properties. When the BN content was greater than 10 vol%, the mechanical properties of Si_3N_4-BN composites decreased significantly due to the very soft properties of BN and the brittle response of the dispersion/matrix interface, resulting in an unacceptably high frictional wear coefficient. HBN is too inert, difficult to interact with the ceramic matrix material, difficult to disperse, and the resulting lubricating film is easy to fall off.

Graphite and boric acid necessitate the presence of moisture or other condensable vapours to facilitate lubrication; otherwise, there is a significant increase in the coefficient of friction (COF). In contrast, MoS_2 demonstrates exceptional low-friction properties in vacuum or dry atmospheres. However, higher humidity levels can result in a two orders of magnitude increase in the COF [137]. When WS_2 is at 500 °C, WO_3 crystal produced by oxidation of WS_2 could be used as lubrication phase [138]. Zhu et al. [139] prepared WS_2/MoS_2 film with good anti-friction and wear resistance. However, due to high sintering temperature of ceramic tool material, the material would decompose and lose its original characteristics [140]. In conclusion, it can be seen that the solid additives need to be used in a suitable environment to avoid the failure of solid additives to enhance the service life of ceramic tool materials. Therefore, among the various influencing factors, the temperature of use is the one that most widely affects the functioning of most solid additives.

3.1. Low-Temperature Friction-Reducing Growth Service Life

The selection of lubricant needs to consider the substrate material and the actual processing scenarios. Various types of solid lubricants and their lubrication mechanisms have been extensively researched, and some scholars have determined through experiments that adding appropriate solid lubricants to certain ceramic substrates in low temperature environments can improve the service life of ceramic cutting tool materials.

Carbon materials such as graphene and carbon nanotubes possess low shear and high protective properties, along with excellent lubrication capabilities. A simulation conducted by Berman et al. [129] demonstrated that at a temperature of 327 °C, the coefficient of friction for graphene can be as small as an extremely low value of 0.005. Xu

et al. [141] demonstrated that the addition of multilayer graphene (MLG) in the test temperature range of 100–550 °C reduced the coefficient of friction and wear rate, and improved the service life. However, at temperatures between 550–600 °C, MLG oxidized and its lubricating effect was substantially weakened. Above 600 °C, MLG lost its lubricating properties. To expand the lubrication range, Ouyang et al. [142] discovered that MLG has significant value for application up to 400 °C by incorporating a lubrication combination of MLG and Ti_3SiC_2 into ZrO_2 (Y_2O_3)-based ceramics. Additionally, Ti_3SiC_2 primarily functions as a lubricant from 400–800 °C, resulting in friction reduction across a wide temperature range. Yuan et al. [143] fabricated $BN_{0.5}C_{0.5}$/fabric composites, harnessing the load-bearing capacity of carbon nanotubes (CNTs) and the self-lubricating effect of boron nitride nanosheets (BNNSs), which exhibited remarkable anti-friction and friction-reducing properties. It was found that, due to the synergistic effect of BNNSs and CNTs, the coefficient of friction and wear rate of the fabric composites were reduced by 32.4% and 64.4%, respectively, thereby improving the material's service life. The study conducted by Choi et al. [130] revealed a decrease in both the amount of wear and coefficient of friction with an increase in the content of carbon nanotubes (CNTs). However, it was observed that beyond 4.5 vol%, there was an increase in both the wear rate and coefficient of friction. It can be seen that the mechanical properties and lubrication effects of materials should be integrated to determine the appropriate amount of solid added lubricant range in order to reduce the wear rate of ceramic tool materials and improve the service life.

The cutting performance of Al_2O_3/TiC/GPLs (ATG) ceramics for dry turning of hardened steels was investigated by Wang et al. [144]. It was found that the tool life of ATG was approximately 125% longer than that of the commercial ceramic tool LT55 and about 174% longer than that of the commercial cemented carbide tool YT15. Wang et al. [145] investigated the cutting performance of a graphene-reinforced Al_2O_3-WC-TiC composite ceramic tool (AWTG0.5). They observed an increase in the tool life of AWTG0.5 tools, primarily attributed to the incorporation of graphene, which enhanced the mechanical properties and wear resistance of the tool. Furthermore, graphene's excellent lubrication and thermal conductivity contribute to reduced friction and temperature in AWTG0.5 tools, thereby mitigating cutting force.

When the temperature exceeds 600 °C, MoO_3 undergoes severe volatilization [146], greatly compromising the long-term stability of the composite. However, it exhibits good lubricity at low temperatures. Some researchers added Mo to the zirconia ceramic matrix, and at 500 °C, the friction coefficient and wear rate of yttria-stabilized quaternary zirconia (3 Y-TZP) with 6 wt%Mo were reduced by 50% and 31%, respectively. At normal operating temperature, the addition of Mo has no obvious effect on the tribological properties. Due to the formation of MoO_3 between friction pairs at high temperature, the friction coefficient is minimum and the specific wear rate is lowest [147]. A novel self-lubricating ceramic cutting insert was developed by MoGhosh et al. [148] through the incorporation of 10 wt% molybdenum (Mo) into zirconia toughened alumina (ZTA). Detailed characterisation revealed the role of molybdenum as a toughened reinforcing material and an increase in fracture toughness of about 5–10% was observed as compared to the ZTA. During high-speed turning of AISI 4340 steel, the new ceramic tool forms a thin lubrication film of molybdenum oxide (MoO_2 and MoO_3) on its surface, successfully resisting wear and extending tool life by 11% compared to popular commercial cutting tools. Su et al. [149] achieved continuous lubrication of Al_2O_3/Mo fiber monolithic ceramics with a microhive weave structure from room temperature to 800 °C using $BaSO_4$. The lubrication mechanism was also analyzed. As shown in Figure 9, when the temperature rises from room temperature to 600 °C, $BaSO_4$ diffuses onto the friction surface during the sliding process, ensuring self-lubrication at this temperature stage (Figure 9a,b). Additionally, when the temperature reaches 800 °C, the Mo boundary oxidizes with O_2 in the air to form MoO_3. At this temperature stage, the formation of both MoO_3 and $BaSO_4$ ensures excellent self-lubrication properties (Figure 9c,d).

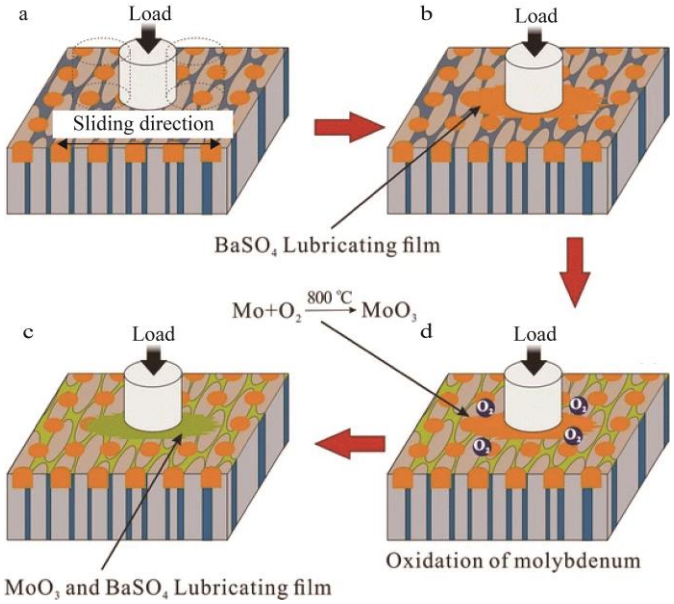

Figure 9. Continuous lubrication mechanism of Al_2O_3/Mo fibre monolithic ceramics [149]: (**a**,**b**) $BaSO_4$ is dragged out and diffused onto the friction surface; (**c**) The Mo reacts with O_2 in the air to form MoO_3; (**d**) MoO_3 and $BaSO_4$ ensure excellent self-lubricating properties.

The WC-30 vol% CBN-5 vol% MoS_2 composites sintered by Wu et al. [150] at 1200 °C and 5.5 GPa exhibited exceptional mechanical properties and self-lubrication characteristics. In comparison to conventional self-lubricating materials, the composite demonstrated a significant increase of at least 52% in hardness (26.3 Gpa) and 46% in fracture toughness (10.5 Mpa $\cdot$ $m^{1/2}$). Regrettably, the reactivity of MoS_2 hindered its performance, while the high wear rate resulted in a substantial enhancement of elastic modulus and reduction of porosity, which were primarily responsible for its outstanding self-lubricating behavior. Wu et al. [151] considered that since MoS_2 had a lower melting point (1185 °C) and decomposition temperature (1300 °C) than ceramic materials, nickel (Ni) coated MoS_2 powder was used as the raw material, which could avoid the oxidation and decomposition of MoS_2 during the spraying process but had less application in the sintering process. It can be seen that surface coating technology can expand the application range of solid additives.

3.2. High-Temperature Friction-Reducing Growth Service Life

As ceramic tool have unique advantages in high-speed cutting, the cutting temperature is generally high during the actual machining process. Therefore, studying the mechanism of reducing friction at high temperatures in the field of ceramic tools is of great significance for their application.

3.2.1. HBN

HBN is commonly utilized as a high-temperature solid lubricant with a graphite-like lamellar structure and exhibits friction-reducing properties from room temperature to 900 °C. The primary mechanism of lubrication is interlaminar slip [152]. Due to its exceptional resistance to high-temperature oxidation and remarkable chemical stability, hBN has been extensively investigated in the field of ceramic tool materials. For example, inhibition of matrix grain growth [153] and reduction of sliding friction [154]. It has been discovered that the main factors influencing the service life of hBN ceramic cutting tool materials are as follows.

I. Firstly, regarding the effect of hBN content. Chen et al. [155] and Li et al. [156] discovered that increasing the hBN content in hBN/SiC and B_4C-hBN composites is beneficial for reducing the friction factor but detrimental to wear resistance. Kuang et al. [157] found that high concentration of hBN would result in low friction coefficient and poor wear resistance of cubic boron nitride (cBN) abrasives. Therefore, an excessive amount of hBN negatively impacts the lifespan of the ceramic material [158].

II. The problem of ambient humidity [159]. Saito et al. [160] studied the sliding properties of sintered hexagonal boron nitride (hBN) in water and found that the friction coefficient of hBN/hBN after sintering decreased to 0.06 in distilled water and 0.23–0.25 in dry air. When the relative humidity is about 50%, the lubrication effect is enhanced and

the wear rate is reduced. This improvement is due to the chemical reaction of hBN with moisture in the spalling pit of the worn surface under wet conditions, resulting in the formation of a discontinuous self-lubricating chemical film [161].

III. Finally, there is the issue of bond strength between hBN and matrix [143]. The influence of hBN and the type of ceramic matrix on the tribological properties of composites was investigated by Sun et al. [162]. The bond strength between hBN and the ceramic matrix was observed to directly influence the exfoliation and spreading of the hBN layer, consequently impacting the formation of friction film and tribological properties of the material.

The tribological behavior of SiC-hBN/SiC ball pair at high temperature was also investigated by Chen et al. [163]. At 800 °C, the wear coefficient and friction coefficient of the SiC-hBN/SiC ball pair were found to be smaller compared to the SiC/SiC ball pair. The bonding strength between hBN and Si_3N_4 is found to be the highest among all materials tested, as illustrated in Figure 10 [162]. Moreover, the friction-induced film exhibits enhanced smoothness and continuity, with no discernible presence of free abrasive particles. The underlying mechanism lies in the robust mutual bonding between Si_3N_4 ceramics and hBN flakes, which effectively facilitates the liberation of hBN within the composite and mitigates the presence of unbound abrasive particles on the frictional interface. The hBN/Al_2O_3 wear surface exhibited a more compact friction film, although a certain amount of free abrasive particles still remained on the abrasive marks. However, the bond strength between ZrO_2 and hBN is relatively low, leading to a loosely adhered friction film on the wear surface that exhibits signs of peeling off, indicating severe abrasive wear characteristics.

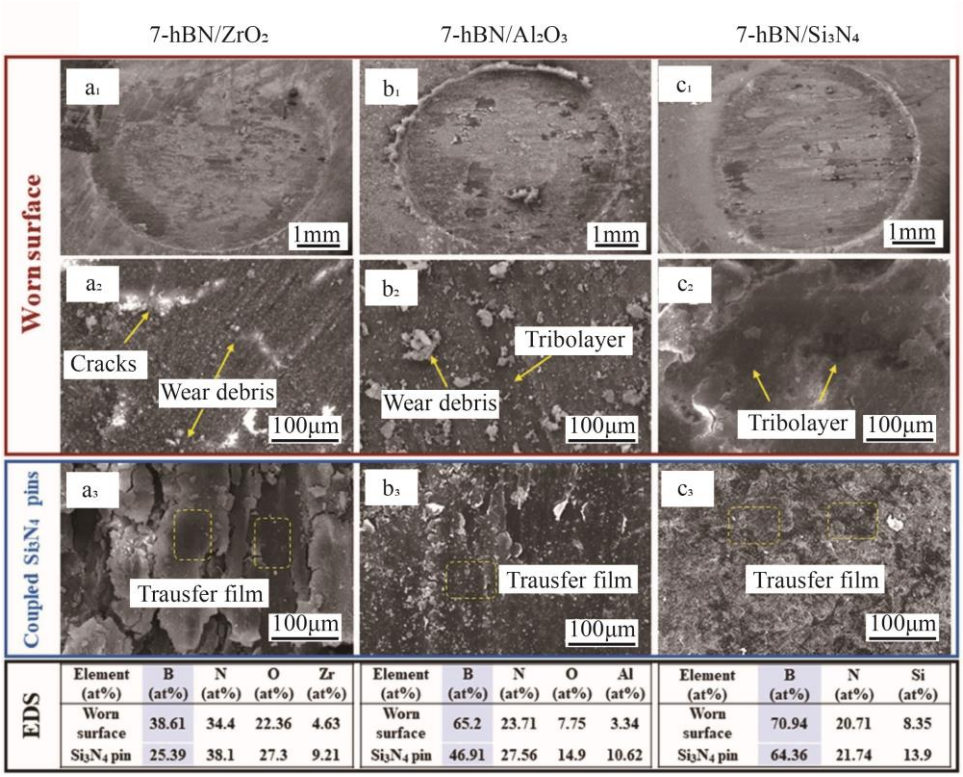

Figure 10. Microstructures of the worn surfaces of the composites and the coupled Si_3N_4 pins together with corresponding EDS analysis: (**a**) the 7-hBN/ZrO_2; (**b**) 7-hBN/Al_2O_3; (**c**) 7-hBN/Si_3N_4 [162]. Reproduced with permission from Elsevier.

To enhance the optimization of the friction film formed on the wear surface of hBN/Al_2O_3, Zhang et al. [76] employed a non-homogeneous nucleation technique for fabricating hBN@Al_2O_3 solid lubricant with a core-shell structure. The hBN@Al_2O_3 particles were uniformly dispersed in the matrix, and the optimal dosage of hBN@Al_2O_3 solid lubricant was determined to be 5%. During the friction wear test, hBN within the hBN@Al_2O_3 particles can be selectively removed to form a robust solid lubrication film on the surface of Al_2O_3/TiC/TiB_2/hBN@Al_2O_3 ceramic cutting tools, thereby significantly mitigating wear and enhancing antiwear properties. Zhang et al. [164] used a heterogeneous nucleation method to encapsulate a dense layer of hexagonal boron nitride (hBN) powder, which is a solid lubricant, on the surface of $Al(OH)_3$. The Si_3N_4/TiC/(hBN@Al_2O_3) self-lubricating ceramic tool materials were meticulously prepared. Microstructural analysis revealed the uniform dispersion and strong bonding of hBN@Al_2O_3 particles within the matrix. The cutting tests demonstrated that the Si_3N_4/TiC/(hBN@Al_2O_3) self-lubricating ceramic tool exhibited superior friction reduction and wear resistance compared to its corresponding counterpart. It can be seen that after adding hBN in appropriate amount and solving the bonding problem between hBN and the substrate with

coating technology, the wear can be significantly reduced and the actual machining life of ceramic tools can be improved. Yin et al. [165] found that the friction coefficients of monolithic Sialon and Sialon- hBN composites were 1.07 and 0.82, respectively. the addition of hBN has a low coefficient of friction and good lubrication, which has an important effect on the tribological properties of the composites. the wear rate of Sialon-hBN composites is slightly lower than that of monolithic Sialon, which improves tool service life.

3.2.2. Metal Oxides

Metal oxides mainly rely on high temperature softening to reduce the coefficient of friction for lubrication [166]. It is worth noting that ceramic tool materials have very high sintering and cutting temperatures. Although some metal oxides have a lubricating effect at certain temperatures [167,168], they decomposed at sintering temperatures. Gassner et al. [167] showed that it was necessary to limit the test temperature to a maximum of 500 °C to inhibit volatilization of oxide MoO_3 in order to exert lubricity. Ouyang et al. [168] found that the plastic deformation, formation and transfer of $BaCrO_4$ lubrication film at high temperature was the main wear mechanism. $BaCrO_4$ acted as an effective solid lubricant above 300 °C, reducing friction and wear of the coating, but it would decompose at the sintering temperature of the ceramic material.

Therefore, it is difficult to achieve the goal of increasing tool life by directly adding them to the ceramic matrix. Metal oxides such as CuO_s, B_2O_3, MnO_2, ZnO can provide a low coefficient of friction to the sliding surface at high temperatures [169,170] and exhibit good stability under high temperature conditions. These properties make them potentially suitable for application in the field of ceramic tool materials.

Copper oxides (CuO_s) are considered potential solid lubricants in many high-temperature applications [171,172]. Valefi et al. [173] and Kong et al. [174] used CuO as a solid lubricant in a zirconia matrix and found that CuO-TZP has a high coefficient of friction and wear rate up to 600 °C, which was attributed to the formation of rough surfaces due to brittle fracture and abrasive wear. However, at temperatures above 700 °C, good self-lubricating properties and anti-wear properties were exhibited. Zirconia toughened alumina (ZTA) ceramic blades doped with CuO solid lubricant were fabricated by the hot pressing process, as reported by Singh et al. [175]. The presence of a copium-rich phase of ionic copper at the grain boundary marginally diminishes the microhardness of the developed sample, while concurrently enhancing fracture toughness through crack bridging and crack deflection phenomena facilitated by the ductile behavior exhibited by Cu particles. The dry processing of AISI 4340 steel revealed that the novel self-lubricating ZTA/CuO composite blade exhibits enhanced cutting performance, demonstrating nearly a 20% reduction in wear on the rear tool face compared to the conventional ZTA blade.

Savchenko et al. [176] prepared WC/Y-TZP-Al_2O_3 hybrid ceramic matrix composite (CMC) by sintering method, and conducted tests at a sliding speed of 7–37 m/s and a contact pressure of 5 MPa. CMC showed low friction and high wear resistance. The excellent tribological properties can be attributed to the in situ mechanochemical formation of ferric tungstate FeW_4 and Fe_2WO_6 on the wear surface of composite specimens. These mixed oxides are contained within multilayer subsurface structures that exhibit easy shear and quasi-viscous behavior, resulting in self-lubricating and self-healing effects during high-speed sliding.

Metal oxides, as one of the main components of ceramic materials, usually exhibit good mechanical properties. The addition of metal oxides as lubricants (friction-reducing phases) has a minimal impact on the mechanical properties. Taking advantage of this, Bas et al. [170] investigated the effect of metal oxide additives on the mechanical properties of Al_2O_3-based or stabilised tetragonal zirconia-based (Y-TZP) ceramics by incorporating a sufficiently small amount (1 or 5 wt%) of solid lubricants such as CuO, ZnO, MgO, MnO_2, and B_2O_3 to maintain the base phase's mechanical properties without increasing the specific wear rate. These selected additives provide a self-lubricating mechanism to reduce dry friction coefficient in ceramic materials' tribological properties. The measured coefficients of friction are presented in Table 2 where it was observed that most tetragonal zirconia (Y-TZP) materials showed no significant change in coefficients except when CuO was added. It can be noted that the effect of CuO addition is dependent on the matrix material; both ceramic materials with CuO addition exhibited low specific wear rates and improved material life span. The authors hypothesized that adding MnO_2, ZnO or B_2O_3 to an Al_2O_3 matrix would enhance its friction-reducing effect and result in lower specific wear rates; while MgO did not appear to act as a lubricant but played an important role in improving structural organization which led to reduced friction and wear while increasing service life for ceramic materials.

Table 2. Coefficient of friction (μ) of ceramic composites during dry-sliding against ceramic ball (α-Al_2O_3 or Y-TZP) [170].

Matrixdisc	Additive	Al_2O_3 Ball (μ)	Y-TZP Ball (μ)
Y-TZP	None	0.70	0.90
	CuO	0.43	0.80
	MnO_2	0.77	–
	MgO	0.85	–
	B_2O_3	0.75	–
Al_2O_3	None	0.55	0.70
	CuO	0.65	0.43
	MnO_2	0.47	–
	MgO	0.48	–
	ZnO	0.49	>0.6
	B_2O_3	0.48	–

Huang et al. [177] prepared self-lubricating ceramic tool materials based on titanium nitride, which exhibited low wear, a low friction coefficient, and a wide temperature range. This solution addressed the issue of short wear failure life in Si_3N_4 ceramics at high temperatures. At low temperatures, the addition of TiN inhibited crack propagation on the wear surface of Si_3N_4 ceramics, significantly reducing their wear rate and overall spalling. At high temperatures, TiN oxidation had self-healing and lubricating effects that greatly improved the wear resistance of Si_3N_4-based ceramics. It is evident that while TiN loses its toughening and strengthening effects at high temperatures [18], it imparts other properties to ceramic tool materials indirectly enhancing their service life.

Chen et al. [146] found that composite ceramics with Al_2O_3 fibers combined with Cr_2O_3 exhibit good friction reduction and wear resistance at high temperatures. As shown in Figure 11a1–e1, the width of the abrasion marks initially decreases with increasing test temperature and is narrowest at 600 °C. Corresponding elemental analyses reveal a significant presence of chromium on the smooth surface, indicating that the Cr_2O_3 phase is dragged to the wear surface to form a continuous lubricating film due to slight plastic deformation and softening. However, poor thermal stability leads to severe cracking of the Cr_2O_3 grain boundaries, resulting in a large number of abrasive grains at 1000 °C and causing severe abrasive wear behavior. The incorporation of alumina fibers contributes to high strength and toughness in the Al_2O_3/Cr_2O_3 fibrous monolithic ceramic, with a maximum crack extension toughness reaching up to 9.05 $MPa \cdot m^{1/2}$. The mechanism is illustrated in Figure 11g–i, where this enhanced toughening behavior can be attributed to crack flexing and branching produced by the bionic layered structure.

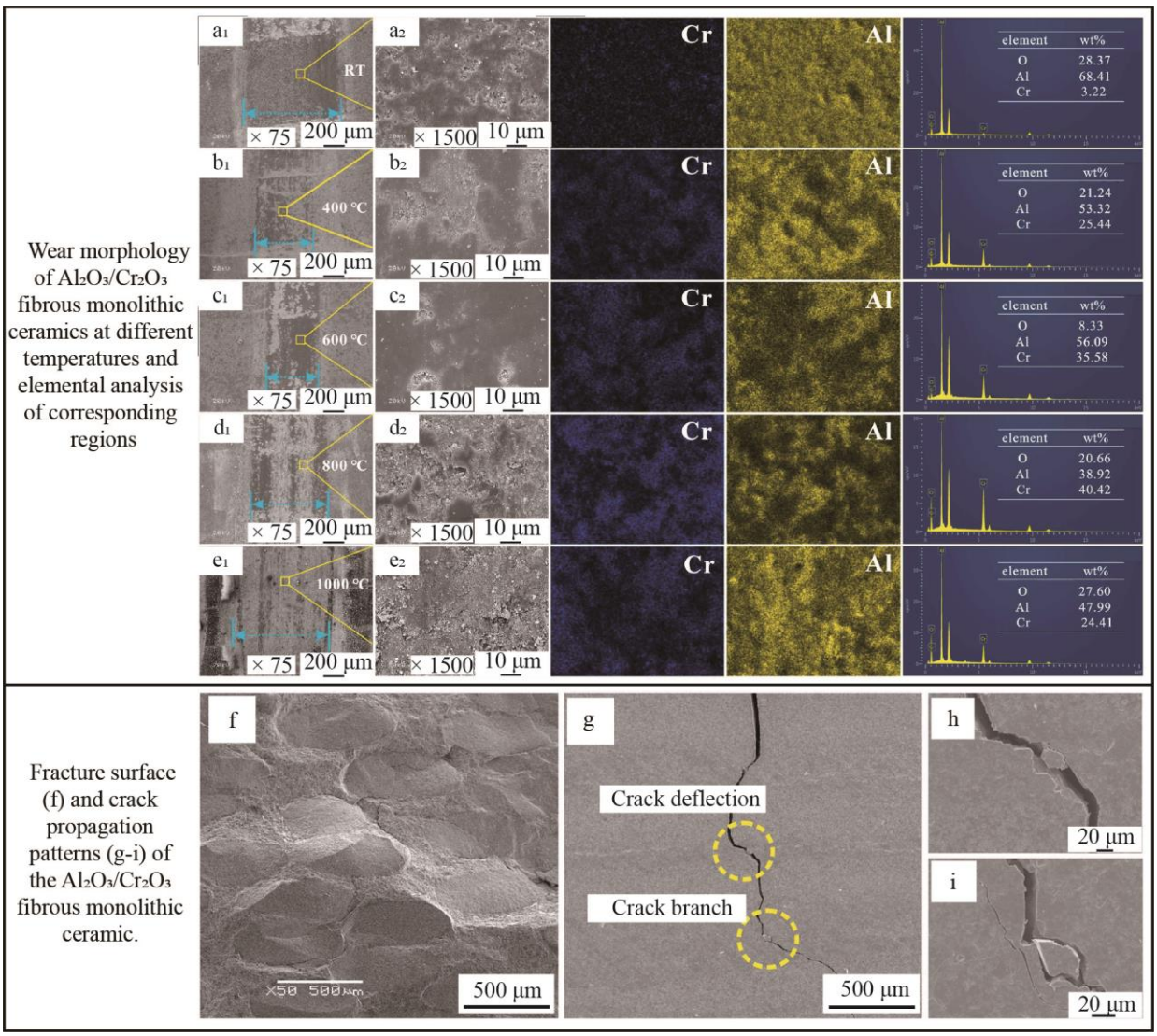

Figure 11. Schematic diagram of toughening and lubrication of Al_2O_3/Cr_2O_3 fibrous monolithic ceramic [146]: The morphologies of the worn surfaces of Al_2O_3/Cr_2O_3 fibrous monolithic ceramics after tribological tests at different temperatures, and the elements distributions of the whole mapped region from images (**a2**,**b2**,**c2**,**d2**,**e2**), as well as corresponding EDS spectrums; Fracture surface (**f**) and crack propagation patterns (**g**–**i**) of the Al_2O_3/Cr_2O_3 fibrous monolithic ceramic. Reproduced with permission from Elsevier.

3.2.3. Alkaline Earth-Metal Fluoride

Similar to metal oxides, the primary lubrication mechanism of alkaline earth metal fluorides is attributed to the softening effect observed at temperatures around 500 °C, which corresponds to the brittle-to-ductile transition occurring at that temperature range [178]. Alkaline earth metal fluorides are widely used as solid lubricants for high temperature processing [179]. Song et al. [180] found that $Al_2O_3/TiC/CaF_2$ self-lubricating ceramic composite had good lubrication wear resistance due to the friction film formed by CaF_2 solid lubricant. Wu et al. [181] and Xu et al. [182] used $Al_2O_3/TiC/CaF_2$ to prepare gradient self-lubricating ceramic tools, solving the problem that the friction and wear resistance of self-lubricating ceramic tools could not be taken into account at the same time. However, it should be noted that their friction reduction capability is poor and they may even increase wear at low temperatures. Ouyang et al. [183] added CaF_2 to a Y_2O_3-stabilized ZrO_2 ceramic matrix and found that CaF_2 lubrication was ineffective at room temperature and increased wear rate. However, when tribological tests were conducted on samples containing CaF_2 up to 800 °C, a significant reduction in wear rate was observed. Liu et al. [184] prepared $Al_2O_3/TiB_2/CaF_2$(ABF) self-lubricating ceramic cutting tool using Al_2O_3/TiB_2 as matrix and CaF_2 as additive. Dry cutting test was conducted on 45 hardened steel at a cutting speed of 120 m/min. The cutting test results showed that the average friction coefficient of the front tool surface was significantly smaller. Deng et al. [185] analyzed SEM micrographs of the wear profiles of Al_2O_3/TiC and $Al_2O_3/TiC/CaF_2$ ceramic tools during machining of hardened steel at 100 m/min for 10 min and found that the $Al_2O_3/TiC/CaF_2$ ceramic tools exhibited less wear and longer life span compared to those without CaF_2 addition. This can be attributed to the fact that under high temperature cutting conditions, CaF_2 in the tool material softens,

precipitates, and disperses on the front face of the tool, resulting in a lower coefficient of friction. However, it should be noted that CaF_2 has poor mechanical properties and its addition needs optimization. Yi et al. [25] proposed a novel intracrystalline self-lubricating nanostructure for the preparation of potential ceramic tool materials. Nano CaF_2 was prepared and used in the synthesis of self-lubricating nano-structured ceramic materials. The incorporation of intracrystalline nanostructures can significantly enhance the tribological properties of materials. The friction coefficient of the material on the 40Cr steel ball ranges from 0.12 to 0.2. When the CaF_2 content was increased from 3.3 vol% to 10 vol%, a noticeable reduction in wear rate was observed, while the change in friction coefficient remained marginal. The wear rate was further increased with the addition of 13.3 vol% CaF_2.

Some researchers coated the surface of CaF_2 with SiO_2 [186,187], Ni [188–190] or Al_2O_3 [191–193] to make up for the problems of low bond strength, difficult dispersion and poor mechanical properties of CaF_2 and the matrix material. Wu et al. [188] found that the microstructure and mechanical properties of the self-lubricating ceramic tool material prepared by adding nickel coated CaF_2 powder were significantly improved compared with the tool material prepared by directly adding uncoated CaF_2 powder. Experiments on dry cutting 45# hardened steel show that the new self-lubricating ceramic tool has better anti-friction wear resistance than the corresponding tool. Chen et al. [194] designed Al_2O_3 /Ti (C, N) /CaF_2@Al_2O_3 self-lubricating ceramic tool materials with different CaF_2@Al_2O_3 contents, and found that core-shell structure improved the bonding strength between solid lubricant and base material, as well as the hardness and fracture toughness of tool material. It is found that with the increase of CaF_2@Al_2O_3 content, the friction coefficient decreases, and the wear increases after the first decrease. Zhang et al. [195] fabricated self-lubricating ceramic tools by substituting CaF_2 with CaF_2@Al_2O_3, effectively mitigating the adverse effects of directly added CaF_2 particles on ceramic tools. They observed that the incorporation of CaF_2@Al_2O_3 resulted in enhanced wear resistance and improved machined surface quality compared to those with direct addition of CaF_2 during the turning process of 40Cr. The optimum content of CaF_2@Al_2O_3 particles was determined to be 10 vol%. The friction reduction and wear resistance mechanism of self-lubricating ceramic tools is illustrated in Figure 12a–d. During the initial stage of cutting, the uniformly distributed CaF_2@Al_2O_3 particles within the ceramic matrix remain in suspension, preventing their precipitation and formation of a lubrication film on the tool surface (Figure 12a). As a result, the flank wear increases rapidly at a cutting distance of 0–200 m (Figure 12e,f). Subsequently, the application of cutting force resulted in the disintegration of the Al_2O_3 shell surrounding CaF_2@Al_2O_3 particles, leading to the exposure of CaF_2 on the surface of the ceramic tool, as depicted in Figure 12b. Furthermore, as illustrated in Figure 12c, precipitation of CaF_2 commenced from the surface of the ceramic tool. However, only a small amount of CaF_2 precipitated at this time, forming an incomplete lubrication film. With the continuous advancement of the cutting process, the cutting temperature continues to rise, so that CaF_2 from the brittle state into a plastic state, the formation of CaF_2 as the main body of the lubrication film on the surface of the tool (Figure 12d). Due to the low shear strength of the lubrication film, it has a good friction reduction effect in the cutting process. As a result, the wear rate of the rear cutter face slows down after the cutting distance reaches 200 m (Figure 12e,f). Through the above analysis, it can be determined that the surface coating technology can make up for the problems of low bonding strength and difficult dispersion of CaF_2 and the base material.

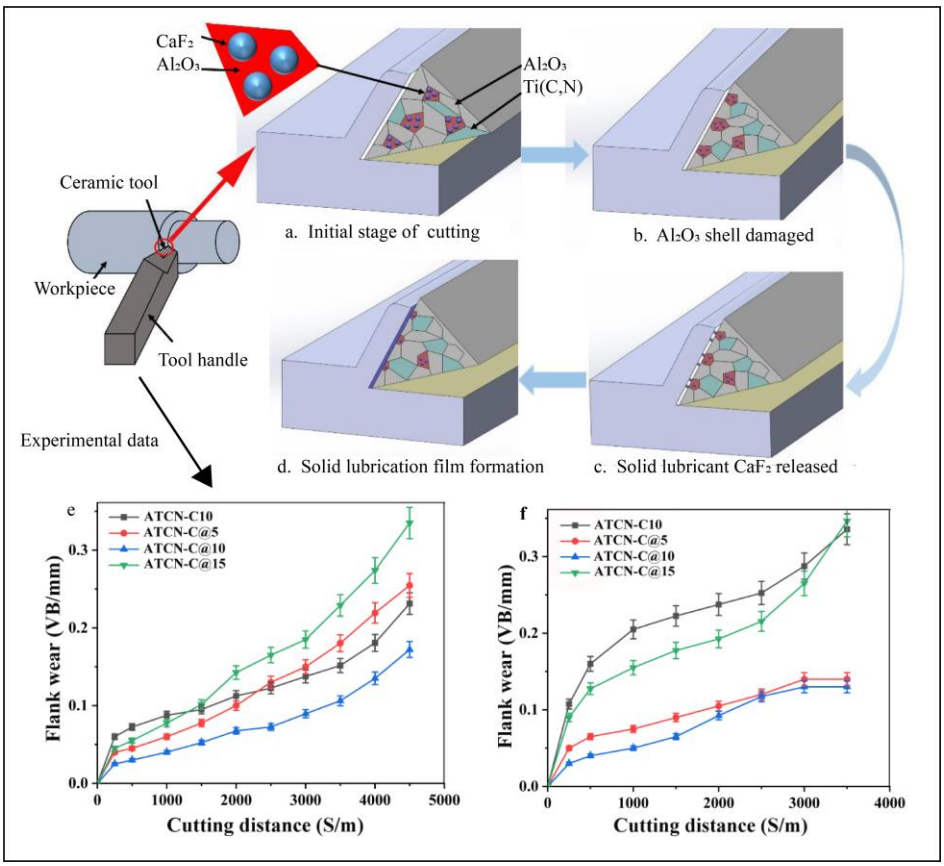

Figure 12. Schematic diagram of solid lubricating film formation process of the ceramic tool with CaF_2@Al_2O_3 added: (**a**–**d**); The flank wear of four ceramic tools at cutting speeds of 100 m/min (**e**) and 300 m/min (**f**) (test conditions: depth of cut a_p = 0.2 mm, feed rates f = 0.102 mm/r) [195].

The wear of partially stabilised ZrO_2-3 mol% Y_2O_3-20 wt% Al_2O_3 (TZ3Y20A) ceramic composites with the addition of CaF_2 and BaF_2 was investigated by J.H. Ouyang et al. [142], as shown in Figure 13. It was observed that the wear increased under ambient conditions but decreased at 800 °C. Specifically, they discovered that adding $BaSO_4$ or $SrSO_4$ to TZ3Y20A reduced the frictional wear rate across a wide temperature range, highlighting the importance of lubricant film formation, plastic deformation, and effective spreading in decreasing frictional wear.

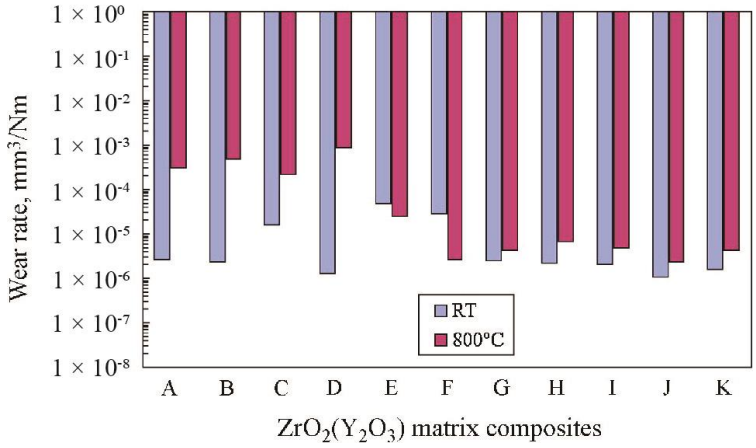

Figure 13. Wear rates of $ZrO_2(Y_2O_3)$ matrix composites incorporated with and with-out solid lubricants at room temperature and 800 °C. (A: TZ3Y; B: TZ3Y20A; C: TZ3Y20A–10Graphite; D: TZ3Y20A–50MoS_2; E: TZ3Y–30CaF_2–10Ag_2O–10Cu_2O; F: TZ3Y20A–31BaF_2–19CaF_2; G: TZ3Y20A–18CaF_2–12CaF_2–30Ag; H: TZ3Y20A–50$BaCrO_4$; I: TZ3Y20A–50$BaSO_4$; J: TZ3Y20A–50$SrSO_4$; K: TZ3Y–50$SrSO_4$–5$CaSiO_3$) [142]. Reproduced with permission from Elsevier.

In order to expand the temperature range at which alkaline earth-metal fluorides reduce friction, Jin et al. [196] discovered that the addition of CaF_2 and Ag significantly decreased the friction factor and wear rate of Al_2O_3 between 200 °C and 650 °C. Bogdanski et al. [197] incorporated the solid lubricants BaF_2/CaF_2 eutectic and silver into a

chromium carbide matrix, where BaF_2/CaF_2 eutectic acted as a high-temperature lubricant above 400 °C, while silver served as a low-temperature lubricant (up to 500 °C).

4. Conclusions

Ceramic tool materials have significant application value in various industries. Solid additives are an effective means of enhancing the service life of ceramic tool materials across a wide range of applications. The properties of solid additives can be utilized to achieve high-quality and efficient machining. This paper reviews the research on solid additives for improving the service life of ceramic tool materials, analyzes the mechanisms of action for different types of solid additives, and discusses precautions for their usage. Based on the characteristics and mechanisms of action, solid additives can be mainly classified into the following types.

(1) Adding one or more of particles, whiskers, rare earth elements and nanoparticles to the matrix material to achieve the goal of toughening and reinforcing can improve the reliability of ceramic cutting tool materials and make ceramic cutting tool materials have a longer service life. Rare earth elements can improve the sintering process, optimise the microstructure of ceramic tool materials and reduce defects. The particle and whisker increase the fracture energy loss by producing crack deflection, crack bridging and other phenomena to improve the reliability of ceramic tool materials.

(2) Part of the toughening and reinforcing materials enables ceramic tool materials to possess self-repair characteristics. When the operating temperature reaches the point of chemical reaction or liquid phase formation, heat can be utilized in the repair process to mend microcracks and surface defects, thereby enhancing the service life of ceramic tool materials. It should be noted that the presence of glassy phase or generated gases in high-temperature environments may have a detrimental effect on tool longevity. The research on the detection, repair and repair efficiency of micro-cracks in cutting process is relatively lacking.

(3) Thermal cracking is an important factor that limits the service life of ceramic tool materials. Friction reduction is an effective means of reducing cutting temperature. Some solid additives possess friction reduction properties, mainly by optimizing the sintering process to improve surface quality of ceramic cutting tool materials and reduce friction, or by forming a lubricating layer between the tool and workpiece to decrease workpiece friction and lower operating temperatures. To achieve the purpose of reducing damage and increasing service life. However, there are certain limitations in applying these solid additives in high-temperature processing due to weak bonding strength with the matrix, low strength, difficulties in dispersion, and susceptibility to decomposition at high temperatures.

As a result of refinements made by researchers, the reliability of ceramic tool materials has significantly increased. The improved service life has led to enhanced machining efficiency, and the properties of solid additives have enabled ceramic tools to be used in an ever-expanding range of operating scenarios. Furthermore, there is still considerable potential (Figure 14).

(1) The combination of multiple solid additives can enhance the performance, application range (e.g., wider lubrication temperature, lower service temperature, resistance to thermal cracking, etc.), and service life of ceramic tool materials. However, due to the complexity of their compositions, it is necessary to pay more attention to the service conditions in order to fully utilize these tools. Further research data is still needed to understand the mechanisms of compositional interactions and synergies. Simulation tools, such as molecular dynamics, can be used to help understand the mechanisms of component interactions and synergies.

(2) Ceramic tool material crack repair phenomenon has great application value and potential. It is still to be explored to improve the repair efficiency of the repair agent, which can be combined with the fluid that can promote the repair to improve the repair efficiency. Exploration and validation of materials to reduce the porosity of repaired surfaces. Micro-crack repair combined with a system that can monitor damage in real time, intuitively determine the repair effect of the cutting process.

(3) Surface cladding technology is an effective means of solving the problems of weak bonding of solid additive phases to the matrix, low strength, and difficulties in dispersion. This allows many solid additives to work with a wider range of ceramic substrate materials, resulting in ceramic tool materials with greater applicability. However there are limitations in the research of various surface capping techniques and further process optimisation is required to increase the yield of capped materials or to improve the quality of capped powders using suitable screening processes. Improve the application value of coated particles in ceramic matrix.

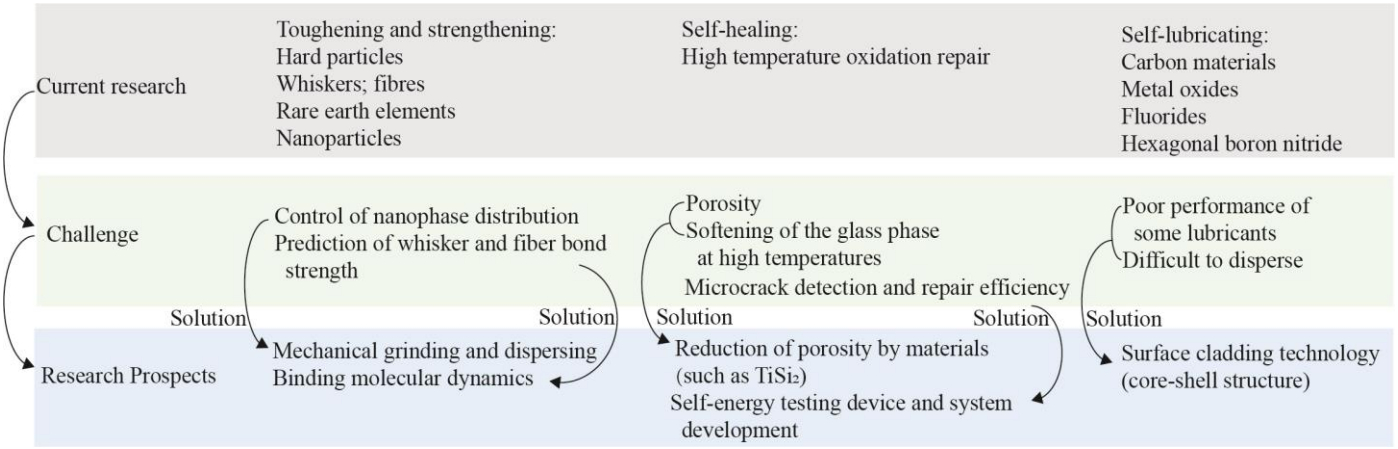

Figure 14. Challenges and prospects for improving the service life of ceramic tool materials with solid additives.

Author Contributions

Conceptualization, B.Z. and W.D.; Methodology, W.D.; Software, Y.S.; Validation, Y.S., B.Z. and W.D.; Investigation, Y.S.; Resources, Y.S.; Data Curation, Y.S.; Writing—Original Draft Preparation, Y.S.; Writing—Review & Editing, B.Z.; Supervision, B.Z.; Project Administration, B.Z.; Funding Acquisition, W.D.

Ethics Statement

Not applicable.

Informed Consent Statement

Not applicable.

Funding

Supported by the National Natural Science Foundation of China (Nos. 92160301, 92060203, 52175415, and 52205475), the Science Center for Gas Turbine Project (No. P2023-B-IV-003-001), the Natural Science Foundation of Jiangsu Province (No. BK20210295), and the Huaqiao University Engineering Research Center of Brittle Materials Machining (MOE, 2023IME-001).

Declaration of Competing Interest

The authors declare that they have no known competing financial interests or personal relationships that could have appeared to influence the work reported in this article.

References

1. Deng JX, Cao TK, Liu LL. Self-lubricating behaviors of Al_2O_3/TiB_2 ceramic tools in dry high-speed machining of hard-ened steel. *J. Eur. Ceram. Soc*. **2005**, *25*, 1073–1079.
2. Huang CZ, Ai X. Development of advanced composite ceramic tool material. *Mater. Res. Bull.* **1996**, *31*, 951–956.
3. Wu H. Toughening and strengthening mechanisms in ceramic nanocomposites. In *Residual Stresses in Composite Materials*; Woodhead Publishing: Sawston, UK, 2021; pp. 279–311.
4. Rahman M, Maeda T, Osada T, Ozaki S. Method of Determining Kinetic Parameters of Strength Recovery in Self-Healing Ceramic Composites. *Materials* **2023**, *16*, 4079.
5. Akhtar SS. A critical review on self-lubricating ceramic-composite cutting tools. *Ceram. Int.* **2021**, *47*, 20745–20767.
6. Furukawa M, Nakano O, Tasashima Y. Fracture toughness of Al_2O_3-TiC ceramics. *Int. J. Refract. Hard Met.* **1988**, *7*, 37–40.
7. Zhang W, Chen Z, Tian C, Wu J, Xiao G, Guo N, et al. Addition of Nano $CaF_2@SiO_2$ and SiC Whiskers in Ceramic Tools for Wear Reduction and Improved Machinability. *Materials* **2022**, *15*, 5430.
8. Shi Y, Chen Z, Ji L, Xiao G, Yi M, Zhang J, et al. Cutting performance and antifriction mechanism of $Al_2O_3/TiC/TiB_2$/h-$BN@Al_2O_3$ self-lubricating ceramic tool. *Int. J. Adv. Manuf. Technol.* **2023**, *125*, 809–818.

9. Akhtar SS. A Systematic Material Design Approach to Develop Self-Lubricating Ceramic-Composite Tool Inserts for Dry Cutting Conditions. In *ASME International Mechanical Engineering Congress and Exposition*; American Society of Mechanical Engineers: New York, NY, USA, 2019.
10. Liu L, Ying G, Jiang Q, Wen D, Wang P, Wu M, et al. Ultra-high-temperature application of MXene: Stabilization of 2D $Ti_3C_2T_x$ for cross-scale strengthening and toughening of 3D TiC. *J. Adv. Ceram.* **2024**, *13*, 1–10.
11. Jia L, Zhang X, Han W, Jin H. The hybrid effect of SiC whisker coupled with -ZrO_2 fiber on microstructure and mechani-cal properties of -ZrB_2-based ceramics. *Mater. Sci. Eng. A* **2012**, *551*, 187–191.
12. Fu Y, Zhang L, Ni X, Liu X, Chen C, Zhao S. Strength-toughening model of eutectic ceramic composite with inherent defects. *Chin. J. Mech. Eng.* **2014**, *27*, 754–760.
13. Zhang L, Sun D, Xiong Y, Liu Y. Toughening mechanism and application analysis of ZrO_2 ceramics under high speed strain condition. *IOP Conf. Ser. Mater. Sci. Eng.* **2019**, *585*, 012014.
14. Yoshitomo OBA, Kyohei TAKEO, Wataru NAKAO, Shingo OZAKI. Numerical study on crack bifurcation of self-healing fiber-reinforced ceramic matrix composite. *Mech. Eng. J.* **2017**, *4*, 16-00705.
15. Chen WH, Nayak PK, Lin HT, Lee AC, Huang JL. Enhanced mechanical properties of WC-reinforced Al_2O_3 ceramics via spark plasma sintering. *Ceram. Int.* **2015**, *41*, 1317–1321.
16. Song J, Jiang L, Liang G, Gao J, An J, Cao L, et al. Strengthening and toughening of TiN-based and TiB_2 -based ceramic tool materials with H_fC additive. *Ceram. Int*. **2017**, *43*, 8202–8207.
17. Yu H, Hou Z, Guo X, Chen Y, Li J, Luo L, et al. Finite element analysis on flexural strength of Al_2O_3-ZrO_2 composite ceramics with different proportions. *Mater. Sci. Eng. A* **2018**, *738*, 213–218.
18. Cheng Y, Zhu T, Sun N, Li Y, Xie Z, Liao N, et al. Synergistic strengthening and toughening of oscillatory pressure sintered WC-ZrO_2-Al_2O_3 ceramics. *J. Alloys Compd*. **2022**, *922*, 166133.
19. Tan Y, Zhang J, Chen P, Zhu Z, Wu S, Tian Z. Zirconia-strengthened yttria ceramics for plasma chamber applications. *Ceram. Int*. **2021**, *47*, 7448–7456.
20. Liu CX, Sun JL, Li G, Li B, Gong F. Fabrication, mechanical properties and fracture behaviors of the laminated Al_2O_3-ZrB_2-MgO/Al_2O_3-TiN-MgO ceramic composite. *Ceram. Int.* **2020**, *46*, 857–865.
21. Yaşar ZA, Celik AM, Haber RA. Improving fracture toughness of B_4C-SiC composites by TiB_2 addition. *Int. J. Refract. Met. Hard Mater.* **2022**, *108*, 105930.
22. Stolin AM, Bazhin PM, Konstantinov AS, Chizhikov AP, Kostitsyna EV, Bychkova MY. Synthesis and characterization of Al_2O_3-ZrO_2-based eutectic ceramic powder material dispersion-hardened with ZrB_2 and WB particles prepared by SHS. *Ceram. Int.* **2018**, *44*, 13815–13819.
23. Nambiraj KM, Rajeswari R, Madhavan S. AlN-TiB_2 based self-lubricating ceramic insert fabricated by spark plasma sintering for dry turning applications. *Mater. Sci. Forum* **2015**, *830–831*, 67–70.
24. Shi Y, Chen H, Chen Z, Huang Y, Zhang R, Tian C, et al. Toughening, reinforcement and repair mechanisms of $TiSi_2$ in Al_2O_3/TiN/$TiSi_2$ ceramics. *Ceram. Int.* **2024**, *50*, 575–583.
25. Yi M, Wang J, Bai X, Xu Y, Xiao G, Chen Z, et al. Synthesis and properties characterization of an Al_2O_3-based ceramic materials with intragranular self-lubricating nanostructure. *Int. J. Refract. Met. Hard Mater.* **2022**, *104*, 105800.
26. Xia T, Tu X, Zhang F, Zhang J, Ren L. In Situ Reaction Strengthening and Toughening of B_4C/$TiSi_2$ Ceramics. *J. Wuhan Univ. Technol. -Mater. Sci. Ed.* **2023**, *38*, 12–19.
27. Grigoriev SN, Fedorov SV, Hamdy K. Materials, properties, manufacturing methods and cutting performance of innovative ceramic cutting tools—A review. *Manuf. Rev.* **2019**, *6*, 19.
28. Deng JX, Ai X. Wear resistance of Al_2O_3/TiB_2 ceramic cutting tools in sliding wear tests and in machining processes. *J. Mater. Process. Technol.* **1997**, *72*, 249–255.
29. Yang Z, Ouyang J, Liu Z. Isothermal oxidation behavior of reactive hot-pressed TiN-TiB_2 ceramics at elevated temperatures. *Mater. Des.* **2011**, *32*, 29–35.
30. Skopp A, Woydt M, Habig KH. Tribological behavior of silicon nitride unlubricated sliding between 22 C materials under and 1000 C. *Wear* **1995**, *181*, 571–580.
31. Ko YM, Kwon WT, Kim YW. Development of Al_2O_3-SiC composite tool for machining application. *Ceram. Int.* **2004**, *30*, 2081–2086.
32. Sun J, Zhao J, Chen Y, Wang L, Yun X, Huang Z. Toughening in low-dimensional nanomaterials high-entropy ceramic nanocomposite. *Compos. Part B Eng.* **2022**, *231*, 109586.
33. Liu Y, Jiang X, Shi J, Luo Y, Tang Y, Wu Q, et al. Research on the interface properties and strengthening–toughening mechanism of nanocarbon-toughened ceramic matrix composites. *Nanotechnol. Rev*. **2020**, *9*, 190–208.

34. Yi MD, Xu CH, Chen ZQ, Wu GY, Xiao GC. Effect of Nano-sized CaF_2 on Mechanical Properties of Self-lubricating Ceramic Material. *J. Chin. Ceram. Soc.* **2014**, *42*, 1127–1133.
35. Mustafa T, Huang J, Gao J, Yan P, Liu Y, Ruiz KH, et al. Nanoplates forced alignment of multi-walled carbon nanotubes in alumina composite with high strength and toughness. *J. Eur. Ceram. Soc*. **2021**, *4*, 5541–5547.
36. Liao N, Jia D, Yang Z, Zhou Y, Li Y, Jia X. Strengthening and toughening effects of MWCNTs on Si_2BC_3N ceramics sintered by SPS technique. *Mater. Sci. Eng. A* **2018**, *71*, 142–150.
37. Xie Z, Jian WR, Tang X, Zhang X, Yao X. Strengthening and toughening mechanisms of metallic glass nanocomposites via graphene nanoplatelets. *J. Non-Cryst. Solids* **2020**, *546*, 120284.
38. Ai YL, Xie XH, He W, Liang BL, Chen WH. Effect of nano-Al_2O_3 on the microstructure and properties of ZrO_2 dental materials prepared by microwave sintering. *Appl. Mech. Mater.* **2014**, *618*, 3–7.
39. Wenya D, Yunlong A. Formation and control of "intragranular" ZrO_2 strengthened and toughened Al_2O_3 ceramics. *Ceram. Int*. **2020**, *46*, 8452–8461.
40. Zhao B, Liu H, Huang C, Wang J, Cheng M, Zhan Q. Evolution mechanisms of high temperature mechanical properties and microstructures of $Al_2O_3/SiC_w/TiC_n$ nanocomposite materials. *J. Alloys Compd.* **2018**, *737*, 46–52.
41. Yin Z, Huang C, Yuan J, Zou B, Liu H, Zhu H. Cutting performance and life prediction of an Al_2O_3/TiC micro-nano-composite ceramic tool when machining austenitic stainless steel. *Ceram. Int.* **2015**, *41*, 7059–7065.
42. Yu H, Li J, Chen Y, Li J, Liu L, Chen X. Analysis of strengthening and toughening mechanisms of bioinspired mineral bridges on hot-pressed alumina-based ceramics through finite element method. *Ceram. Int.* **2019**, *4*, 11251–11257.
43. Zhu N, Zhang L, Wen G, Hou Y. Effect of SiC whiskers on the mechanical properties of polymer-derived ceramics prepared by digital light processing and its strengthening and toughening mechanism. *J. Alloys Compd.* **2023**, *968*, 171852.
44. Chen S, Fan H, Su Y, Li J, Song J, Hu L, et al. Bioinspired PcBN/hBN fibrous monolithic ceramic: High-temperature crack resistance responses and self-lubricating performances. *J. Adv. Ceram.* **2022**, *11*, 1391–1403.
45. Wang A, Wang S, Yin H, Bai R, Liu J, Zhang Z, et al. Structural effects in 'brick-and-mortar'architecture: Bio-inspired ceramic matrix composites developed through a new method. *Ceram. Int.* **2023**, *49*, 5042–5048.
46. Xiong Y, Wang W, Ye Z, Yang J, Zhao Y, Huang J. Strengthening and toughening of Ti_5Si_3 by TiC-coated short carbon fiber: Fabrication, interfacial control, and mechanism of reinforcement. *J. Eur. Ceram. Soc*. **2023**, *4*, 3988–3997.
47. Lang Y, Wang CA. Al_2O_3-fiber-reinforced porous YSZ ceramics with high mechanical strength. *Ceram. Int.* **2014**, *40*, 10329–10335.
48. Kim RY, Pagano NJ. Crack Initiation in Unidirectional Brittle-Matrix Composites. *J. Mater. Sci.* **1991**, *74*, 1082–1090.
49. Garrett KW, Bailey JE. Multiple transverse fracture in 90 cross-ply laminates of a glass fibre-reinforced polyester. *J. Mater. Sci.* **1977**, *12*, 157–168.
50. Meyer P, Waas AM. Mesh-objective two-scale finite element analysis of damage and failure in ceramic matrix composites. *Integr. Mater. Manuf. Innov.* **2015**, *4*, 63–80.
51. Gao X, Fang G, Song Y. Hysteresis loop model of unidirectional carbon fiber-reinforced ceramic matrix composites under an arbitrary cyclic load. *Compos. Part B Eng.* **2014**, *56*, 92–99.
52. Yang C, Jiao G, Wang B. Effect of interfacial properties on tensile strength of ceramic matrix composites. *J. Inorg. Mater.* **2009**, *24*, 919–923.
53. Guo R, Li Z, Li L, Zheng R, Ma C. Toughening mechanism and oxidation resistance of SiC whisker-toughened SiAlCN ceramics. *Ceram. Int.* **2024**, *5*, 8853–8864.
54. Liu H, Yin Z, Zheng L, Yuan J. Spark plasma sintering of Al_2O_3/SiC_w ceramic end mill: Grain growth kinetics, mechanical properties and cutting performance. *Ceram. Int.* **2023**, *49*, 38683–38690.
55. Li Z, Guo R, Li L, Zheng R, Ma C. Microstructure and fracture toughness of SiAlCN ceramics toughened by SiC_w or GNPs. *Ceram. Int*. **2023**, *49*, 29709–29718.
56. Zhao B, Liu H, Huang C, Wang J, Cheng M. Fabrication and mechanical properties of Al_2O_3-SiC_w-TiC_{np} ceramic tool material. *Ceram. Int.* **2017**, *43*, 10224–10230.
57. Zhang X, Liu C, Li M, Zhang J. Research on toughening mechanisms of alumina matrix ceramic composite materials improved by rare earth additive. *J. Rare Earths* **2008**, *26*, 367–370.
58. Rezaee S, Ranjbar K, Kiasat AR. Characterization and strengthening of porous alumina-20 wt% zirconia ceramic composites. *Ceram. Int*. **2020**, *46*, 893–902.
59. Hassan AM, Naga SM, Awaad M. Toughening and strengthening of Nb_2O_5 doped zirconia/alumina (ZTA) composites. *Int. J. Refract. Met. Hard Mater.* **2015**, *48*, 338–345.
60. Xu CH, Huang CZ, Ai X. Toughening and strengthening of advanced ceramics with rare earth additives. *Ceram. Int.* **2006**, *32*, 423–429.
61. Xu CH, Ai X. Applications of rare earth elements in nitride ceramic materials. *Mater. Rev.* **1997**, *11*, 46–50.

62. Xu CH, Ai X, Huang CZ. Applications of rare earth elements in oxide, carbide and boride ceramic materials. *Bull. Chin. Ceram. Soc*. **1998**, *17*, 64–68.
63. Chae KW, Kim DY. Effect of Y_2O_3 addition on the densification of an Al_2O_3-TiC composite. *J. Am. Ceram. Soc.* **1993**, *76*, 1857–1862.
64. Xu CH, Ai X, Huang CZ. Mechanical property and cutting performance of yttrium reinforced Al_2O_3/Ti(C,N) composite ceramic tool material. *J. Mater. Eng. Perform.* **2001**, *10*, 102–107.
65. Lumby RJ, Butler E, Lewis MH. Lucas Syalons: Composition, Structure, Properties and Uses. In *Progress in Nitrogen Ceramics*; Springer: Dordrecht, The Netherlands, 1983; pp. 683–694.
66. Choi JH, Lee SM, Nahm S, Kim S. Effect of Y_2O_3 content on the microstructural characteristics and the mechanical and thermal properties of Yb-doped SiAlON ceramics. *Ceram. Int*. **2022,** *48*, 12161–12169.
67. Guanming Q, Xikum L, Tai Q, Haitao Z, Honghao Y, Ruiting M. Application of rare earths in advanced ceramic materials. *J. Rare Earths* **2007**, *25*, 281–286.
68. Xu C, Zhang Y, Wu G, Wang X, Zhang H. Rare earth ceramic cutting tool and its cutting behavior when machining hardened steel and cast iron. *J. Rare Earth*s **2010**, *28*, 492–496.
69. Yuan S, Fan H, Amin M, Zhang C, Guo M. A cutting force prediction dynamic model for side milling of ceramic matrix composites C/SiC based on rotary ultrasonic machining. *Int. J. Adv. Manuf. Technol.* **2016**, *86*, 37–48.
70. Wang R, Li W. Determining fracture strength and critical flaw of the ZrB_2-SiC composites on high temperature oxidation using theoretical method. *Compos. Part B Eng.* **2017**, *129*, 198–203.
71. Lange FF, Gupta TK. Crack healing by heat treatment. *J. Am. Ceram. Soc.* **1970**, *53*, 54–55.
72. Park SM, O'Boyle DR. Observations of crack healing in sodium chloride single crystals at low temperatures. *J. Mater. Sci.* **1977**, *12*, 840–841.
73. Choi SR, Tikare V. Crack healing of alumina with a residual glassy phase: Strength, fracture toughness and fatigue. *Mater. Sci. Eng. A* **1993**, *171*, 77–83.
74. Powers JD, Glaeser AM. High-Temperature Healing of Cracklike Flaws in Titanium Ion-Implanted Sapphire. *J. Am. Ceram. Soc.* **1993**, *76*, 2225–2234.
75. Lv J, Zheng Z, Ding H, Jin Z. Self-healing of surface cracks in alumina-based ceramic composites. *J. Inorg. Mater*. **2001**, *03*, 535–540.
76. Zhang S, Xiao G, Chen Z, Ji L, Xu C, Yi M, et al. Mechanical properties, microstructure and crack healing ability of Al_2O_3/TiC/TiB_2/h-BN@Al_2O_3 self-lubricating ceramic tool material. *Ceram. Int*. **2021**, *47*, 14551–14560.
77. Gupta TK. Crack healing in thermally shocked MgO. *J. Am. Ceram. Soc.* **1975**, *58*, 143.
78. Gupta TK. Crack healing and strengthening of thermally shocked alumina. *J. Am. Ceram. Soc.* **1976**, *59*, 259–262.
79. Zhou G, Gu Q, Sun H, Zhou K, Yu S, Zhou K, et al. High-temperature self-healing behavior of reaction-bonded silicon carbide porous ceramic membrane supports. *J. Eur. Ceram. Soc*. **2024**, *44*, 1959–1971.
80. Ruggles-Wrenn MB, Lee MD. Fatigue behavior of an advanced SiC/SiC ceramic composite with a self-healing matrix at 1300 °C in air and in steam. *Mater. Sci. Eng. A* **2016**, *677*, 438–445.
81. Li L, Reynaud P, Fantozzi G. Cyclic-dependent damage evolution in self-healing woven SiC/[Si-B-C] ceramic-matrix composites at elevated temperatures. *Materials* **2020**, *13*, 1478.
82. Ebel A, Caty O, Rebillat F. Effect of temperature on static fatigue behavior of self-healing CMC in humid air. *Compos. Part A Appl. Sci. Manuf.* **2022**, *157*, 106899.
83. Buyakov A, Shmakov V, Buyakova S. Dual composite architectonics: Fracture toughness and self-healing of ZrB_2–SiC–TaB_2 based UHTC. *Ceram. Int.* **2023**, *49*, 13648–13656.
84. Zgalat-Lozynskyy O, Kud I, Ieremenko L, Krushynska L, Zyatkevych D, Grinkevych K, et al. Synthesis and spark plasma sintering of Si_3N_4–ZrN self-healing composites. *J. Am. Ceram. Soc.* **2022**, *42*, 3192–3203.
85. Maruoka D, MurakaMi T, Kasai E. Influence of heat treatment temperature on self-healing effect of Fe particle/Mullite ceramic composites. *Tetsu-To-Hagane* **2020**, *106*, 844–850.
86. Lee KS, Ahn H, Lee GW, Sloof WG. Self-healing of indentation damage in Ti_2AlC MAX phase ceramics. *Mater. Lett*. **2023**, *334*, 133683.
87. Farle A, Kwakernaak C, Zwaag SVD, Sloof WG. A conceptual study into the potential of $M_{n+1}AX_n$-phase ceramics for self-healing of crack damage. *J. Eur. Ceram. Soc*. **2015**, *35*, 37–45.
88. Wu X, Chen T, Wang B, Song Y, Huang Q, Huang Z. Preparation of self-healing C_f/SiBCN (O) composite using a novel polyborosilazane. *Ceram. Int.* **2022**, *48*, 31738–31745.
89. Maruoka D, Nanko M. High-temperature oxidation and self-healing behavior of SiC and Ni Co-dispersed into Al_2O_3 matrix composite. *Ceram. Int.* **2023**, *49*, 28629–28634.

90. Mersagh Dezfuli S, Sabzi M. A study on the effect of presence of CeO_2 and benzotriazole on activation of self-healing mechanism in ZrO_2 ceramic-based coating. *Int. J. Appl. Ceram. Technol.* **2018**, *15*, 1248–1260.
91. Zhang N, Asle Zaeem M. Nanoscale self-healing mechanisms in shape memory ceramics. *Npj Comput. Mater.* **2019**, *5*, 54.
92. Chu MC, Cho SJ, Park HM. Crack-healing in reaction-bonded silicon carbide. *Mater. Lett.* **2004**, *58*, 1313–1316.
93. Houjou K, Ando K, Liu SP, Sato, S. Crack-healing and oxidation behavior of silicon nitride ceramics. *J. Eur. Ceram. Soc*. **2004**, *24*, 2329–2338.
94. Wang B, Tu R, Wei Y, Cai H. Self-healing of SiC-Al_2O_3-B_4C Ceramic Composites at Low Temperatures. *Materials* **2022**, *15*, 652.
95. Yoshioka S, Nakao W. Methodology for evaluating self-healing agent of structural ceramics. *J. Intell. Mater. Syst. Struct.* **2014**, *26*, 1395–1403.
96. Burlachenko AG, Mirovoy YA, Dedova ES, Buyakova SP. Self-healing in high temperature ZrB_2-SiC ceramics. *AIP Conf. Proc.* **2019**, *2167*, 020042.
97. Monteverde F, Saraga F, Reimer T, Sciti D. Thermally stimulated self-healing capabilities of ZrB_2-SiC ceramics. *J. Eur. Ceram. Soc*. **2021**, *41*, 7423–7433.
98. Dedova ES, Burlachenko AG, Mirovoy YA, Buyakov AS, Buyakova SP. Self-healing in ZrB_2-ZrC-SiC-ZrO_2 ceramics. *AIP Conf. Proc.* **2019**, *2167*, 020067.
99. Kim BS, Ando K, Chu MC, Saito S. Crack-healing behavior of monolithic alumina and strength of crack-healed member. *J. Soc. Mater. Sci. Jpn*. **2003**, *52*, 667–673.
100. Song Q, Zhang Z. Microstructure and self-healing mechanism of B_4C-TiB_2-SiC composite ceramic after pre-oxidation behaviour. *Ceram. Int.* **2022**, *48*, 25458–25464.
101. Ando K, Furusawa K, Takahashi K, Sato S. Crack-healing ability of structural ceramics and a new methodology to guarantee the structural integrity using the ability and proof-test. *J. Eur. Ceram. Soc*. **2005**, *25*, 549–558.
102. Chlup Z, Flasar P, Kotoji A, Dlouhy I. Fracture behaviour of Al_2O_3/SiC nanocomposite ceramics after crack healing treatment. *J. Eur. Ceram. Soc*. **2008**, *28*, 1073–1077.
103. Lee SK, Takahashi K, Yokouchi M, Suenaga H, Ando K. High-temperature fatigue strength of crack-healed Al_2O_3 toughened by SiC whiskers. *J. Eur. Ceram. Soc*. **2004**, *87*, 1259–1264.
104. Lin J, Huang Y, Zhang H. Crack healing and strengthening of SiC whisker and ZrO_2 fiber reinforced ZrB_2 ceramics. *Ceram. Int*. **2014**, *40*, 16811–16815.
105. Li M, Huang C, Zhao B, Liu H, Wang J, Liu Z. Crack-healing behavior of Al_2O_3-TiB_2-$TiSi_2$ ceramic material. *Ceram. Int*. **2018**, *44*, 2132–2137.
106. Huang M, Li Z, Wu J, Khor KA, Huo F, Duan F, et al. Multifunctional Alumina Composites with Toughening and Crack-Healing Features Via Incorporation of NiAl Particles. *J. Am. Ceram. Soc.* **2015**, *98*, 1618–1625.
107. Takahashi K, Yokouchi M, Lee SK, Ando K. Crack-healing behavior of Al_2O_3 toughened by SiC whiskers. *J. Am. Ceram. Soc.* **2003**, *86*, 2143–2147.
108. Liu JC, Yang ZF. Effect of Heat Treatment on Structure and Properties of Mullite/ZrO_2/SiC_p Composite Ceramics. *J. Tianjin Univ.* **1998**, *31*, 638–643.
109. Sun J, Liu C, Zhang R, Gong F, Wang C, Li G. Comprehensive effect of the mechanical properties, laminated structure and healing conditions on the self-healing behaviors of laminated Al_2O_3-MgO ceramic composites. *Ceram. Int*. **2019**, *45*, 13597–13604.
110. Moffatt J, Plumbridge W, Herman R. High temperature crack annealing effects on fracture toughness of alumina and alumina-SiC composite. *Br. Ceram. Trans.* **1996**, *95*, 23–29.
111. Savchenko NL, Mirovoy YA, Buyakov AS, Burlachenko AG, Rudmin MA, Sevostyanova IN, et al. Adaptation and self-healing effect of tribo-oxidizing in high-speed sliding friction on ZrB_2-SiC ceramic composite. *Wear* **2020**, *446–447*, 203204.
112. Cui H, Chen ZQ, Xiao GC, Ji L, Yi M, Zhang J, et al. Mechanical Properties and Microstructures of Al_2O_3/TiC/TiB_2 Ceramic Tool Material. *Crystals* **2021**, *11*, 637.
113. Zhao B, Liu H, Huang C, Wang J, Wang B, Hou Y. Cutting performance and crack self-healing mechanism of a novel ceramic cutting tool in dry and high-speed machining of Inconel 718. *Int. J. Adv. Manuf. Technol.* **2019**, *102*, 3431–3438.
114. Ozaki S, Osada T, Nakao W. Finite element analysis of the damage and healing behavior of self-healing ceramic materials. *Int. J. Solids Struct.* **2016**, *100*, 307–318.
115. Ozaki S, Yamamoto J, Kanda N, Osada T. Kinetics-based constitutive model for self-healing ceramics and its application to finite element analysis of Alumina/SiC composites. *Open Ceram.* **2021**, *6*, 100135.
116. Maeda T, Osada T, Ozaki, S. Novel numerical approach for reliability-assurance of ceramics by combining self-crack-healing with proof testing. *J. Eur. Ceram. Soc*. **2024**, *44*, 2261–2270.

117. Bellezza G, Couégnat G, Ricchiuto M, Vignoles GL. A 2D image-based multiphysics model for lifetime evaluation and failure scenario analysis of self-healing ceramic-matrix mini-composites under a tensile load. *J. Eur. Ceram. Soc*. **2022**, *42*, 6391–6403.
118. Nakao W, Hayakawa T, Yanaseko T, Ozaki S. Advanced Fiber Reinforced Self-Healing Ceramics for Middle Range Temperature. *Key Eng. Mater.* **2019**, *810*, 119–124.
119. Greil P. Self-healing engineering ceramics with oxidation-induced crack repair. *Adv. Eng. Mater.* **2020**, *22*, 1901121.
120. Huang J, Guo L, Zhong L. Synergistic healing mechanism of self-healing ceramics coating. *Ceram. Int*. **2022**, *48*, 6520–6527.
121. Altin A, Nalbant M, Taskesen A. The effects of cutting speed on tool wear and tool life when machining Inconel 718 with ceramic tools. Materials & design. *Mater. Des.* **2007**, *28*, 2518–2522.
122. Dorri-Moghadam A, Schultz BF, Ferguson J, Omrani E, Rohatgi PK, Gupta N. Functional metal matrix composites: Self-lubricating, self-healing, and nanocomposites-an outlook. *Jom-Us* **2014**, *66*, 872–881.
123. Rohatgi P, Ray S, Liu Y. Tribological properties of metal matrix-graphite particle composites. *Int. Mater. Rev.* **1992**, *37*, 129–152.
124. Liu Y, Lim S, Ray S, Rohatgi P. Friction and wear of aluminium-graphite composites: The smearing process of graphite during sliding. *Wear* **1992**, *159*, 201–205.
125. Muratore C, Voevodin AA. Molybdenum disulfide as a lubricant and catalyst in adaptive nanocomposite coatings. *Surf. Coat. Technol.* **2007**, *28*, 2518–2522.
126. Liu E, Gao Y, Jia J, Bai Y. Friction and wear behaviors of Ni-based composites containing graphite/Ag_2MoO_4 lubricants. *Tribol. Lett.* **2013**, *50*, 313–322.
127. Liu EY, Wang WZ, Gao YM, Jia JH. Tribological properties of adaptive Nibased composites with addition of lubricious Ag_2MoO_4 at elevated temperatures. *Tribol. Lett.* **2012**, *47*, 21–30.
128. Parveez B, Wani MF, Ali MF, Banday S, Mir MJ, Mushtaq S. Tribological Characterization of Iron Based Ceramic Reinforced Self-lubricating Material. *J. Phys. Conf. Ser.* **2019**, *1240*, 012108.
129. Berman D, Deshmukh SA, Sankaranarayanan SKRS, Erdemir A, Sumant AV. Macroscale superlubricity enabled by graphene nanoscroll formation. *Science* **2005**, *348*, 1118–1122.
130. Choi HJ, Lee SM, Bae DH. Wear characteristic of aluminum-based composites containing multi-walled carbon nanotubes. *Wear* **2010**, *270*, 12–18.
131. Chen Z, Guo N, Xu C, Ji L, Guo R, Wang B. Synthesis and Simulation of CaF_2@ Al $(OH)_3$ Core-Shell Coated Solid Lubricant Composite Powder. *Crystals* **2019**, *9*, 578.
132. Ji L, Chen Z, Guo R, Xu C, Guo N. Preparation of nano—Coating powder CaF_2@$Al(OH)_3$ and its application in Al_2O_3/Ti(C,N) self-lubricating ceramic tool materials. *Ceram. Int.* **2020**, *46*, 15949–15957.
133. Zhou J, Cheng Y, Wan Y, Chen H, Wang Y, Ma K, et al. Enhancement mechanisms of self-lubricating Ti_3SiC_2 ceramic doping in CoCrFeNi high-entropy alloy via high-speed laser cladding: Tribology and electrochemical corrosion. *Surf. Coat. Technol.* **2024**, *480*, 130554.
134. Carrapichano JM, Gomes JR, Silva RF. Tribological behaviour of Si_3N_4-BN ceramic materials for dry sliding applications. *Wear* **2002**, *253*, 1070–1076.
135. Baradeswaran A, Perumal AE. Study on mechanical and wear properties of Al7075/Al_2O_3/graphite hybrid composites. *Compos. Part B Eng.* **2014**, *56*, 464–471.
136. Su Y, Zhang Y, Song J, Hu L. Tribological behavior and lubrication mechanism of self-lubricating ceramic/metal composites: The effect of matrix type on the friction and wear properties. *Wear* **2017**, *372*, 130–138.
137. Peterson MB, Murray SF, Florek JJ. Consideration of lubricants for temperatures above 1000 F. *ASLE Trans.* **1959**, *2*, 225–234.
138. Zhu J, Zeng Q, He W, Zhang B, Yan C. Elevated-temperature super-lubrication performance analysis of dispersion-strengthened WSN coatings: Experimental research and first-principles calculation. *Surf. Coat. Technol.* **2021**, *406*, 126651.
139. Zhu L, Wang C, Wang H, Xu B, Zhuang D, Liu J, et al. Microstructure and tribological properties of WS_2/MoS_2 multilayer films. *Appl. Surf. Sci*. **2012**, *258*, 1944–1948.
140. Su Y, Zhang Y, Song J, Hu L. Novel Approach to the Fabrication of an Alumina-MoS_2 Self-Lubricating Composite via the In Situ Synthesis of Nanosized MoS_2. *ACS. Appl. Mater. Interfaces* **2017**, *9*, 30263–30266.
141. Xu Z, Zhang Q, Jing P, Zhai W. High-temperature tribological performance of TiAl matrix composites reinforced by multilayer graphene. *Tribol. Lett.* **2015**, *58*, 1–9.
142. Ouyang JH, Li YF, Wang YM, Zhou Y, Murakami T, Sasaki S. Microstructure and tribological properties of ZrO_2 (Y_2O_3) matrix composites doped with different solid lubricants from room temperature to 800 °C. *Wear* **2009**, *267*, 1353–1360.

143. Yuan J, Zhang Z, Yang M, Wu L, Li P, Guo F, et al. Coupling hybrid of BN nanosheets and carbon nanotubes to enhance the mechanical and tribological properties of fabric composites. *Compos. Part A Appl. Sci. Manuf.* **2019**, *123*, 132–140.
144. Wang J, Cheng Y, Zhang Y, Yin Z, Hu X, Yuan Q. Friction and wear behavior of microwave sintered Al_2O_3/TiC/GPLs ceramic sliding against bearing steel and their cutting performance in dry turning of hardened steel. *Ceram. Int.* **2017**, *43*, 14827–14835.
145. Wang X, Zhao J, Gan Y, Tang X, Gai S, Sun X. Cutting performance and wear mechanisms of the graphene-reinforced Al_2O_3-WC-TiC composite ceramic tool in turning hardened 40Cr steel. *Ceram. Int.* **2022**, *48*, 13695–13705.
146. Chen S, Su Y, Sun Q, Fan H, Song J, Hu L, Zhang Y. Strong, tough and high temperature self-lubricated fibrous monolithic ceramic in Al_2O_3/Cr_2O_3 system. *Tribol. Int.* **2022**, *172*, 107646.
147. Dai J, Li S, Zhang H. Microstructure and wear properties of self-lubricating TiB_2-TiC_xN_y ceramic coatings on Ti-6Al-4V alloy fabricated by laser surface alloying. *Surf. Coat. Technol.* **2019**, *369*, 269–279.
148. Kong L, Bi Q, Zhu S, Qiao Z, Yang J, Liu W. Effect of CuO on self-lubricating properties of ZrO_2(Y_2O_3)-Mo composites at high temperatures. *J. Eur. Ceram.Soc.* **2014**, *34*, 1289–1296.
149. Su Y, Hu L, Fan H, Song J, Zhang Y. Surface Engineering Design of Alumina/Molybdenum Fibrous Monolithic Ceramic to Achieve Continuous Lubrication from Room Temperature to 800 °C. *Tribol. Lett.* **2017**, *65*, 2.
150. Wu J, Wang H, Zhang Z, Wang C, Hou Z, Wan S, et al. High-pressure synthesis and performance analysis of WC-cBN-MoS_2 self-lubricating ceramic composites. *Int. J. Refract. Met. Hard Mater.* **2023**, *110*, 105989.
151. Wu Z, Li S, Fan X, Vogel F, Mao J, Tu X. In-situ preparation of robust self-lubricating composite coating from thermally sprayed ceramic template. *J. Adv. Ceram.* **2023**, *12*, 357–372.
152. Martin JM, Le MT, Chassagnette C, Gardos MN. Friction of hexagonal boron nitride in various environments. *Tribol. Trans.* **1992**, *35*, 462–472.
153. Xu XG, Xu CH, Fang B, Wang CL, Yi MD. Preparation and mechanical properties of TiB_2/WC/h-BN self-lubricating ceramic material. *J. Mater. Eng.* **2011**, *1*, 63–67.
154. Skopp A, Woydt M. Ceramic and ceramic composite materials with improved friction and wear properties. *Tribol. Trans.* **1995**, *38*, 233–242.
155. Chen J, Chen J, Wang S, Sun Q, Cheng J, Yu Y, et al. Tribological properties of h-BN matrix solid-lubricating composites under elevated temperatures. *Tribol. Int.* **2020**, *148*, 106333.
156. Li X, Gao Y, Wei S, Yang Q, Zhong Z. Dry sliding tribological properties of self-mated couples of B_4C-hBN ceramic composites. *Ceram. Int.* **2017**, *43*, 162–166.
157. Kuang WJ, Zhao B, Yang CY, Ding WF. Effects of h-BN particles on the microstructure and tribological property of self-lubrication CBN abrasive composites. *Ceram. Int.* **2020**, *46*, 2457–2464.
158. Ding, H. Research on friction and wear performance of TiB_2 based self-lubricating ceramic composites. *MATEC Web Conf.* **2017**, *100*, 04009.
159. Chen W, Zhang D, Lv Z, Li H. Self-lubricating mechanisms via the in situ formed tribo-film of sintered ceramics with hBN addition in a high humidity environment. *Int. J. Refract. Met. Hard Mater.* **2017**, *66*, 163–173.
160. Saito T, Honda F. Chemical contribution to friction behavior of sintered hexagonal boron nitride, in water. *Wear* **2000**, *237*, 253–260.
161. Li X, Gao Y, Yang Q, Pan W, Li Y, Zhong Z, et al. Evaluation of tribological behavior of B_4C-hBN ceramic composites under water-lubricated condition. *Ceram. Int.* **2015**, *41*, 7387–7393.
162. Sun Q, Song J, Chen S, Shi J, Zhang X, Su Y, et al. Tribological behavior and lubrication mechanism of h-BN/ceramic composites: Effects of h-BN platelet size and ceramic phase. *Tribol. Int.* **2023**, *187*, 108722.
163. Chen Z, Li H, Fu Q, Qiang X. Tribological behaviors of SiC/h-BN composite coating at elevated temperatures. *Tribol. Int.* **2012**, *56*, 58–65.
164. Zhang W, Yi M, Xiao G, Ma J, Wu G, Xu C. Al_2O_3-coated h-BN composite powders and as-prepared Si_3N_4 -based self-lubricating ceramic cutting tool material. *Int. J. Refract. Met. Hard Mater.* **2018**, *71*, 1–7.
165. Yin L, Zhao K, Ding Y, Wang Y, He Z, Huang S. Effect of hBN addition on the fabrication, mechanical and tribological properties of Sialon materials. *Ceram. Int.* **2022**, *48*, 7715–7722.
166. Suszko T, Gulbiński W, Jagielski J. The role of surface oxidation in friction processes on molybdenum nitride thin films. *Surf. Coat. Technol.* **2005**, *194*, 319–324.
167. Gassner G, Mayrhofer PH, Kutschej K, Mitterer C, Kathrein M. Magnéli phase formation of PVD Mo–N and W–N coatings. Surface and Coatings Technology. *Surf. Coat. Technol.* **2006**, *201*, 3335–3341.
168. Ouyang JH, Sasaki S, Umeda K. The friction and wear characteristics of low-pressure plasma-sprayed ZrO_2-$BaCrO_4$ composite coating at elevated temperatures. *Surf. Coat. Technol.* **2002**, *154*, 131–139.

169. Ali E, Li SH, Jin YS. Relation of certain quantum chemical parameters to lubrication behavior of solid oxides. *Int. J. Mol. Sci*. **2005**, *6*, 203–218.
170. Kerkwijk B, García M, Van Zyl WE, Winnubst L, Mulder EJ, Schipper DJ, et al. Friction behaviour of solid oxide lubricants as second phase in α-Al_2O_3 and stabilised ZrO_2 composites. *Wear* **2004**, *256*, 182–189.
171. Valefi M, Rooij M, Schipper DJ, Winnubst L. Effect of temperature on friction and wear behaviour of CuO-zirconia composites. *J. Eur. Ceram. Soc*. **2012**, *32*, 2235–2242.
172. Huang H, Wang L, Qi Q, Tang H, Li T, Yang Y, et al. Titanium nitride induced wide temperature range self-lubricating silicon nitride ceramics with low wear and stable low friction coefficient. *Mater. Today Commun.* **2024**, *39*, 108729.
173. Hussain MS, Goswami S, Ghosh K, Kumar P, Mandal N. Evaluation of mechanical and tribological characteristics of hot-pressed self-lubricating CuO/MgO/ZTA ceramic composites. *Mater. Today Proc.* **2022**, *50*, 2522–2527.
174. Singh BK. State-of-Art on Self-Lubricating Ceramics and Application of Cu/CuO as Solid Lubricant Material. *Trans. Indian Ceram. Soc.* **2023**, *82*, 1–13.
175. Singh BK, Goswami S, Ghosh K, Roy H. Mandal N. Performance evaluation of self lubricating CuO added ZTA ceramic inserts in dry turning application. *Int. J. Refract. Met. Hard Mater.* **2021**, *98*, 105551.
176. Savchenko N, Sevostyanova I, Grigoriev M, Sablina T, Buyakov A, Rudmin M, et al. Self-Lubricating Effect of WC/Y–TZP–Al_2O_3 Hybrid Ceramic–Matrix Composites with Dispersed Hadfield Steel Particles during High-Speed Sliding against an HSS Disk. *Lubricants* **2022**, *10*, 140.
177. Ghosh K, Goswami S, Prajapati PK, Roy P, Mandal, N. Pressure-less sintering of molybdenum-reinforced ceramic cutting inserts with improved tool life. *Int. J. Refract. Met. Hard Mater.* **2024**, *120*, 106619.
178. Ouyang JH, Shi CC, Liu ZG, Wang YM, Wang YJ. Fabrication and high-temperature tribological properties of self-lubricating NiCr-$BaMoO_4$ composites. *Wear* **2015**, *330*, 272–279.
179. Xu CH, Wu GY, Xiao GC, Fang B. Al_2O_3/(W,Ti)C/CaF_2 multi-component graded self-lubricating ceramic cutting tool material. *Int. J. Refract. Met. Hard Mater.* **2014**, *45*, 125–129.
180. Song P, Yang X, Wang S, Yang L. Tribological properties of self-lubricating laminated ceramic materials. *J. Wuhan Univ. Technol. -Mater. Sci. Ed.* **2014**, *29*, 906–911.
181. Wu G, Xu C, Xiao G, Yi M, Chen Z. Structure design of Al_2O_3/TiC/CaF_2 multicomponent gradient self-lubricating ceramic composite and its tribological behaviors. *Ceram. Int.* **2018**, *44*, 5550–5563.
182. Xu C, Xiao G, Zhang Y, Fang B. Finite element design and fabrication of Al_2O_3/TiC/CaF_2 gradient self-lubricating ceramic tool material. *Ceram. Int.* **2014**, *40*, 10971–10983.
183. Ouyang JH, Sasaki S, Murakami T, Umeda K. The synergistic effects of CaF_2 and Au lubricants on tribological properties of spark-plasma-sintered ZrO_2 (Y_2O_3) matrix composites. *Mater. Sci. Eng. A* **2004**, *386*, 234–243.
184. Jianxin D, Tongkun C, Xuefeng Y, Jianhua L. Self-lubrication of sintered ceramic tools with CaF_2 additions in dry cutting. *Int. J. Mach. Tools Manuf.* **2006**, *46*, 957–963.
185. Liu J, Zhou H, Zhou W, Deng J, Zhang G, Zhou Y. Self-lubricating Ceramic Cutting Tool with Solid Lubricant based and a Double-situ Reaction Mechanism. *China Mech. Eng.* **2016**, *27*, 2069.
186. Chen Z, Guo N, Ji L, Xu C. Synthesis of CaF_2 Nanoparticles Coated by SiO_2 for Improved Al_2O_3/TiC Self-Lubricating Ceramic Composites. *Nanomaterials* **2019**, *9*, 1522.
187. Li Q, Xiao G, Chen Z, Guo N, Yi M, Zhang J, et al. Self-lubricating ceramic tool materials synergistically toughened by nano-coated particles and silicon carbide whiskers. *Int. J. Refract. Met. Hard Mater.* **2021**, *98*, 105560.
188. Wu G, Xu C, Xiao G, Yi M, Chen Z, Xu L. Self-lubricating ceramic cutting tool material with the addition of nickel coated CaF_2 solid lubricant powders. *Int. J. Refract. Met. Hard Mater.* **2016**, *56*, 51–58.
189. Wu G, Xu C, Xiao G, Yi M. Recent Progress in Self-Lubricating Ceramic Composites. In *Self-Lubricating Composites*; Springer: Berlin, Germany, 2018; pp. 133–154.
190. Wu G, Xu C, Xiao G, Yi M, Chen Z, Chen H. An advanced self-lubricating ceramic composite with the addition of core-shell structured h-BN@Ni powders. *Int. J. Refract. Met. Hard Mater.* **2018**, *72*, 276–285.
191. Chen Z, Ji L, Guo N, Guo R. Mechanical properties and microstructure of Al_2O_3/TiC based self-lubricating ceramic tool with CaF_2@$Al(HO)_3$. *Int. J. Refract. Met. Hard Mater.* **2018**, *75*, 50–55.
192. Chen Z, Ji L, Guo R, Xu C, Li Q. Mechanical properties and microstructure of Al_2O_3/Ti(C,N)/CaF_2@Al_2O_3 self-lubricating ceramic tool. *Int. J. Refract. Met. Hard Mater.* **2019**, *80*, 144–150.
193. Chen Z, Guo N, Ji L, Guo R. An advanced self-lubricating ceramic composite with the addition of core-shell structured CaF_2@Al_2O_3 powders. *Int. J. Appl. Ceram. Technol.* **2018**, *16*, 753–760.
194. Chen Z, Guo N, Ji L, Guo R, Xu C. Influence of CaF_2@Al_2O_3 on the friction and wear properties of Al_2O_3/Ti(C,N)/CaF_2@Al_2O_3 self-lubricating ceramic tool. *Mater. Chem. Phys.* **2019**, *223*, 306–310.

195. Zhang S, Xiao G, Chen Z, Xu C, Yi M, Li Q, et al. Influence of $CaF_2@Al_2O_3$ on Cutting Performance and Wear Mechanism of Al_2O_3/Ti(C,N)/$CaF_2@Al_2O_3$ Self-Lubricating Ceramic Tools in Turning. *Materials* **2020**, *13*, 2922.
196. Jin Y, Koji K, Noritsugu U. Tribological properties of self-lubricating CMC/Al_2O_3 pairs at high temperature in air. *Tribol. Lett.* **1998**, *4*, 243–250.
197. Bogdanski MS, Sliney HE, Dellacorte C. The effect of processing and compositional changes on the tribology of PM212 in air. In Proceedings of the 1993 STLE Annual Meeting, E-7462, Calgary, Alberta, 17–20 May 1993.